



**HAL**  
open science

## Identification of new binding partners of the chemosensory signaling protein G $\gamma$ 13 expressed in taste and olfactory sensory cells.

Zhenhui Liu, Claire Fenech, Hervé Cadiou, Sylvie Grall, Esmerina Tili, Fabienne Laugerette, Anna Wiencis, Xavier Grosmaître, Jean-Pierre Montmayeur

► **To cite this version:**

Zhenhui Liu, Claire Fenech, Hervé Cadiou, Sylvie Grall, Esmerina Tili, et al.. Identification of new binding partners of the chemosensory signaling protein G $\gamma$ 13 expressed in taste and olfactory sensory cells.. *Frontiers in Cellular Neuroscience*, 2012, 6, pp.26. 10.3389/fncel.2012.00026 . hal-00716694

**HAL Id: hal-00716694**

**<https://u-bourgogne.hal.science/hal-00716694>**

Submitted on 11 Jul 2012

**HAL** is a multi-disciplinary open access archive for the deposit and dissemination of scientific research documents, whether they are published or not. The documents may come from teaching and research institutions in France or abroad, or from public or private research centers.

L'archive ouverte pluridisciplinaire **HAL**, est destinée au dépôt et à la diffusion de documents scientifiques de niveau recherche, publiés ou non, émanant des établissements d'enseignement et de recherche français ou étrangers, des laboratoires publics ou privés.



Distributed under a Creative Commons Attribution 4.0 International License



# Identification of new binding partners of the chemosensory signaling protein G $\gamma$ 13 expressed in taste and olfactory sensory cells

Zhenhui Liu<sup>1††</sup>, Claire Fenech<sup>1†</sup>, Hervé Cadiou<sup>2†</sup>, Sylvie Grall<sup>1</sup>, Esmerina Tili<sup>1†</sup>, Fabienne Laugerette<sup>3</sup>, Anna Wiencis<sup>3</sup>, Xavier Grosmaître<sup>2</sup> and Jean-Pierre Montmayeur<sup>1,3\*</sup>

<sup>1</sup> Chemosensory Perception, Centre des Sciences du Goût et de l'Alimentation, UMR-6265 CNRS, UMR-1324 INRA, Dijon, France

<sup>2</sup> Functional Plasticity of Olfactory Neurons, Centre des Sciences du Goût et de l'Alimentation, UMR-6265 CNRS, UMR-1324 INRA, Dijon, France

<sup>3</sup> General Olfaction and Sensing Program on a European Level, Centre des Sciences du Goût et de l'Alimentation, UMR-6265 CNRS, UMR-1324 INRA, Dijon, France

## Edited by:

Dieter Wicher, Max Planck Institute for Chemical Ecology, Germany

## Reviewed by:

Monika Stengl, Universität Kassel, Germany

Yuanquan Song, University of California San Francisco, USA

## \*Correspondence:

Jean-Pierre Montmayeur,  
Chemosensory Perception, Unités Mixtes de Recherche, Centre des Sciences du Goût, 9E Boulevard J. D'Arc, 21000 Dijon, France.  
e-mail: jean-pierre.montmayeur@u-bourgogne.fr

## † Present address:

Zhenhui Liu, Marine Life College, Ocean University of China, 5 Yushan Road, 266003 Qingdao, China.  
Hervé Cadiou, Nociception and Pain Department, Institut des Neurosciences Cellulaires et Intégratives (INCI), CNRS UPR3212, 5 Rue Blaise Pascal, F-67084 Strasbourg, France.

Esmerina Tili, Ohio State University, Comprehensive Cancer Center, 460 West 12th Ave, BRT 1060, Columbus, OH 43201, USA.

† These authors contributed equally to this work.

Tastant detection in the oral cavity involves selective receptors localized at the apical extremity of a subset of specialized taste bud cells called taste receptor cells (TRCs). The identification of the genes coding for the taste receptors involved in this process have greatly improved our understanding of the molecular mechanisms underlying detection. However, how these receptors signal in TRCs, and whether the components of the signaling cascades interact with each other or are organized in complexes is mostly unexplored. Here we report on the identification of three new binding partners for the mouse G protein gamma 13 subunit (G $\gamma$ 13), a component of the bitter taste receptors signaling cascade. For two of these G $\gamma$ 13 associated proteins, namely GOPC and MPDZ, we describe the expression in taste bud cells for the first time. Furthermore, we demonstrate by means of a yeast two-hybrid interaction assay that the C terminal PDZ binding motif of G $\gamma$ 13 interacts with selected PDZ domains in these proteins. In the case of the PDZ domain-containing protein zona occludens-1 (ZO-1), a major component of the tight junction defining the boundary between the apical and baso-lateral region of TRCs, we identified the first PDZ domain as the site of strong interaction with G $\gamma$ 13. This association was further confirmed by co-immunoprecipitation experiments in HEK 293 cells. In addition, we present immunohistological data supporting partial co-localization of GOPC, MPDZ, or ZO-1, and G $\gamma$ 13 in taste buds cells. Finally, we extend this observation to olfactory sensory neurons (OSNs), another type of chemosensory cells known to express both ZO-1 and G $\gamma$ 13. Taken together our results implicate these new interaction partners in the sub-cellular distribution of G $\gamma$ 13 in olfactory and gustatory primary sensory cells.

**Keywords:** taste bud, ZO-1, G $\gamma$ 13, PDZ, olfactory sensory neurons, MPDZ, GOPC

## INTRODUCTION

In rodents the peripheral gustatory system contributes to the detection of sapid molecules present in the oral cavity. This task is accomplished through taste receptors present on the apical microvilli of specialized polarized neuroepithelial taste bud cells also called taste receptor cells (TRCs) or type II cells. TRCs are one of four cell types found in the taste buds of the tongue papillae along with supporting cells (type I), presynaptic cells (type III) and basal cells (type IV) (Finger, 2005). TRCs are elongated cells extending microvilli at their apical end. These extensions which protrude from the adjacent epithelium at the taste bud pore harbor taste receptors designed to recognize the sapid compounds dissolved in saliva. At the pore, tight junctions between the cells composing the taste bud bestow polarity on the cells and seal the paracellular space thus isolating taste receptors on the apical

membrane from ion channels found on the basolateral membrane. TRPM5 and voltage-gated Na<sup>+</sup> channels are the main types of channels found on the baso-lateral membrane of TRCs (Gao et al., 2009) where they are thought to play an important role in the generation of action potentials coding the properties of the tastants (Vandenbeuch and Kinnamon, 2009). Claudins and occludins are two of the main transmembrane proteins composing the tight junction (Furuse et al., 1998; Tsukita and Furuse, 1998). The selectivity of the paracellular barrier formed by tight junctions between neighboring cells is defined by the specific nature of the claudins composing it (Tsukita et al., 2008). It was reported recently that claudin 6 and 7 are found in microvilli and on the basolateral membrane of a subset of taste bud cells (TBCs) respectively while claudin 4 and 8, which are associated with a reduced cationic conductance, are prevalent at the taste

bud pore (Michlig et al., 2007). These proteins interact with zona occludens-1 (ZO-1), a multimodular cytoplasmic protein (Mitic and Anderson, 1998). ZO-1 was the first protein (225 kDa) shown to be specifically associated with the tight junction (Anderson et al., 1988; Stevenson and Keon, 1998). Subsequent studies identified ZO-1 isoforms as well as ZO-2 and ZO-3 as binding partners of ZO-1 (Gumbiner et al., 1991). ZO proteins belong to the large family of membrane-associated guanylate kinases (MAGUKs). All three known ZO proteins are each composed of three PDZ domains, one Src homology 3 domain (SH3), one guanylate kinase-like homologue domain (GUK) and proline-rich domains. PDZ and GUK domains interact selectively with claudins and occludins respectively (Furuse et al., 1994; Itoh et al., 1999). In addition, ZO proteins can bind to actin thus acting as scaffolds linking tight-junction proteins to the cytoskeleton (Fanning et al., 1998).

PDZ domains are typically stretches of about 100 amino acids able to recognize selectively a short peptide motif. Their role in receptor clustering and the organization of supramolecular complexes is well documented (Sheng, 1996). MPDZ also known as MUPP1, is a 13 PDZ domains-containing protein interacting selectively with a great number of PDZ binding motif-containing proteins including claudin-1 (Hamazaki et al., 2002). Single or multiple PDZ domains-containing proteins are often involved in the trafficking and localization of receptors or cytosolic signaling proteins to specialized membrane regions. A well-studied such example is the Golgi-associated protein GOPC also known as PIST. GOPC contains a single PDZ domain and two coiled-coil domains, one of which includes a leucine zipper important for homodimerization. It is known to regulate the intracellular sorting and plasma membrane location of a number of proteins (Yao et al., 2001; Cheng et al., 2002; Gentsch et al., 2003; Hassel et al., 2003; Wente et al., 2005; Ito et al., 2006) including the adherent junction protein cadherin 23 in the highly specialized sensory hair cells of the inner ear (Xu et al., 2010).

In TRCs, bitter tastants binding to the apical membrane or membrane depolarization both lead to the secretion of adenosine 5'-triphosphate (ATP) from gap junction hemichannels located on the baso-lateral membrane (Huang and Roper, 2010). The signaling cascade downstream of taste G protein-coupled receptors (GPCRs) involves a number of well-characterized components. One of these signaling molecules is a G protein alpha subunit called gustducin (G $\alpha$ gust) which plays an important role in sweet, umami, and bitter taste transduction (Gilbertson et al., 2000; He et al., 2004). Gustducin is part of a heterotrimeric complex including G beta 1 (G $\beta$ 1) and G $\gamma$ 13, consequently G $\gamma$ 13 much like G $\alpha$ gust is abundant in a subset of type II TRCs (Huang et al., 1999; Clapp et al., 2001; Ohtubo and Yoshii, 2011). Expression of G $\gamma$ 13 has also been reported in three additional types of sensory cells including retinal bipolar cells, vomeronasal, and olfactory sensory neurons (VOSNs and OSNs) (Huang et al., 2003; Kulaga et al., 2004; Kerr et al., 2008). More recently nutrient-sensing neurons of the hypothalamus were found to express G $\gamma$ 13 as well (Ren et al., 2009). In OSNs G $\gamma$ 13 is very abundant in cilia along with G $\alpha$ Olf and the guanine nucleotide exchange factor Ric-8B to which it was revealed to bind *in vitro* (Kerr et al., 2008). In TRCs, G $\gamma$ 13 was reported to interact directly with the

PDZ-containing scaffolding proteins PSD95, Veli-2, and SAP97 (Li et al., 2006).

Here, we report the identification of three new interaction partners for G $\gamma$ 13 with various subcellular distributions in taste cells and OSNs. Through these previously unidentified interactions our results highlight partnerships between signal transduction components and multimodular proteins implicated in macromolecular complexes with possible consequences on sensory signaling.

## MATERIALS AND METHODS

### ANIMALS

Experiments were performed on C57BI/6J mice (P0—7 weeks old). The animals were fed a standard laboratory chow ad libitum (UAR A04, Usine d'Alimentation Rationnelle, France) and housed under constant temperature and humidity with a light-dark cycle of 12 h following French guidelines for the use and care of laboratory animals. All experimental protocols were approved by the animal ethics committee of the University of Burgundy.

### EXPRESSION CONSTRUCTS

Mice were euthanized with an overdose of sodium pentobarbital and decapitated. Various tissues were collected and immediately processed for total RNA isolation using the RNAeasy kit (Qiagen, Germany) following the manufacturer's instructions. The RNA was then treated with DNase I (Promega, USA) and cleaned before reverse transcription. First strand cDNA was synthesized using 1  $\mu$ g of total RNA with Superscript II (Invitrogen, USA) according to the manufacturer's protocol.

The entire open reading frame of mouse G $\gamma$ 13, PDZ domains of ZO-1, Veli-2, PSD95, SAP97, RGS12, SH3 domain of ZO-1, and c-terminal intracellular regions of the junctional adhesion molecule (JAM), claudin 1, claudin 4, or claudin 8 were PCR amplified from C57BI/6J mice brain, testis, or circumvallate papillae cDNA using specific primers (Operon, Germany) containing a Sal I (forward primer) or Not I (reverse primer) restriction site. For a complete list of primers including melting temperatures and size of the expected PCR products see **Table A1**.

PCR reactions (25  $\mu$ l) contained 1 $\times$  PFU turbo buffer (Stratagene, USA), 0.4  $\mu$ M of each primer, 10  $\mu$ M dNTPs (Qiagen, Germany) and 1/20th of the appropriate RT reaction (water for control). Cycling parameters were: 95°C for 2 min then 35 cycles of 95°C for 30 s; appropriate melting temperature (**Table A1**) for 40 s, 72°C for 60 s, and final elongation at 72°C for 10 min. Following amplification (Biometra, Germany) an aliquot of the PCR products was loaded onto 1.4% agarose Seakem TAE gels (Cambrex, USA) to verify the specificity of the reaction. Single products of the expected size were then subcloned into pSTBlue-1 according to the manufacturer's directions (Novagen, USA). Recombinant clones were analyzed for accuracy by sequencing before subsequent subcloning into the Sal I and Not I sites of either pDBLeu (bait) or pEXP (prey) vectors of the Proquest two-hybrid system (Invitrogen, USA) or pDisplay-FLAG or pDisplay-HA (Invitrogen, USA) vectors. All constructs were sequenced to ensure in frame subcloning.

## YEAST TWO-HYBRID INTERACTIONS

Yeast two-hybrid interactions were performed following the recommendations of the manufacturer of the Proquest two-hybrid system (Invitrogen, USA). Briefly, the appropriate combination of bait and prey plasmids (200 ng each) were co-transformed into competent MaV203 yeast cells (Invitrogen, USA) and plated onto minimal media plates without leucine and tryptophan. The plates were incubated for 48 h at 30°C before selection of two colonies, each dissolved into 500 ml of water. To test the strength of the interaction 10 μl of each slurry was spotted side by side onto plates lacking leucine, histidine, and tryptophan but containing either 0 (control plate), 12.5, 25, or 50 mM 3-Amino-1,2,4-triazole (3-AT) (Sigma, USA). After 24 h at 30°C, the plates were replica cleaned using a velour cloth and incubated an additional 48–72 h at 30°C prior to growth assessment.

## CO-IMMUNOPRECIPITATION AND WESTERN BLOTTING

For co-immunoprecipitation assays with full length ZO-1 and Gγ13, 4 μg of a pcDNA3-FLAG-Gγ13 construct (generous gift of B. Malnic) were co-transfected into HEK 293 cells (60 mm dish) using Lipofectamine LTX (Invitrogen, USA) together with 4 μg of either pcDNA3, full-length pCB6-MYC-ZO-1 or a truncated pCB6-MYC-ZO-1 lacking the PDZ1 domain (pCB6-MYC-ZO-1mut) (generous gift of A. Fanning). pcDNA3-FLAG-Gγ13 + pCB6-MYC-ZO-1 or pcDNA3-FLAG-Gγ13 + pCB6-MYC-ZO-1mut transfections were performed in parallel. Two days later the transfected cells were lysed on ice in 600 μl lysis buffer containing 20 mM Tris, pH 8.0, 150 mM NaCl, 2 mM EDTA, 1% Triton X-100, 0.05% SDS, 1 mg/ml bovine serum albumin, 1 mM DTT and Complete protease inhibitor cocktail (Roche, Switzerland). The lysates were incubated 20 min on ice, centrifuged at 14,000 rpm in a microcentrifuge for 20 min at 4°C and the supernatant incubated overnight at 4°C with 5 μg of mouse monoclonal anti-FLAG (Kodak, USA). Antibody/proteins complexes were recovered with 50 μl protein G-coupled dynabeads (Invitrogen, USA) according to manufacturer's instructions. After three consecutive washes in PBS buffer containing Ca<sup>2+</sup> and Mg<sup>2+</sup> the samples were eluted by heating to 80°C for 10 min in LDS sample buffer (Invitrogen, USA) and subjected to SDS-PAGE and Western blot analysis.

For co-immunoprecipitation assays with full length Gγ13 and truncated forms of ZO-1, 3.5 μg of a pDisplay-HA-Gγ13 construct was co-transfected into HEK 293 cells plated on 60 mm dishes using Lipofectamine LTX (Invitrogen, USA) together with 3.5 μg of either pDisplay or various truncated forms of ZO-1, Veli-2, or PSD95 into pDisplay-FLAG. Forty-eight hours later cells were lysed on ice in 600 μl lysis buffer containing 25 mM Hepes, pH 7.5, 5 mM MgCl<sub>2</sub>, 4 mM EDTA, 1% Triton X-100, and Complete protease inhibitor cocktail (Roche, Switzerland). Protein extracts were treated essentially as described above except that 8 μg 12CA5 mouse monoclonal anti-HA antibody (Roche, Switzerland) were used for immunoprecipitation.

For Western blotting, IP products or total protein lysates (30 μg) were typically separated on a denaturing 4–12% Bis-Tris PAGE gel (Invitrogen, USA), transferred onto a hybond-P, PVDF membrane (GE Healthcare, USA) and incubated overnight at 4°C with the appropriate primary antibody. Mouse monoclonal

anti-HA (1/400; Roche, USA) or anti-FLAG (1/1000; Kodak, USA) or rabbit polyclonal anti-Ezrin H-276 (1/500; Santa Cruz, USA) or mouse monoclonal anti-myc tag 9B11 (1/1000; Cell Signaling Technology, USA). The membrane was subsequently processed using the SNAP id system (Millipore, USA) and signal was detected with an HRP-coupled secondary antibody and a chemiluminescent substrate (Supersignal West Pico, Pierce, USA) on a Chemidoc imager (Biorad, USA). Quantification and normalization was performed using ImageLab (Biorad, USA). When necessary membranes were stripped using a stripping solution (Uptima, USA) and reprobbed with another primary antibody.

To analyze the expression of the PDZ domain-containing proteins and test the specificity of the antibodies used for immunohistochemistry circumvallate papillae and whole olfactory epithelia of fifteen 6–8 weeks old C57Bl/6J mice were collected and pooled together. Tissue lysates were prepared in lysis buffer using a tissue lyser (Qiagen, Germany) during three cycles of 90 s each at 20 Hz. After centrifugation the soluble fraction was recovered and the protein content assessed. Seventy-five microgram of each lysate were separated on denaturing 4–12% Bis-Tris PAGE gel (Invitrogen, USA), transferred onto a hybond-P, PVDF membrane (GE Healthcare, USA) and incubated overnight at 4°C with the appropriate primary antibody. Mouse monoclonal anti-β-actin (1/1000; A5441; Sigma, USA), or rabbit polyclonal anti-GOPC (1/500; SAB3500332, Sigma, USA), or rabbit polyclonal anti-ZO-1 (1/600; 40–2200; Invitrogen, USA), or mouse monoclonal anti-MPDZ (1/250; 611558; BD Transduction Laboratories, USA), or goat polyclonal anti-Gγ13 (1/200; sc-26781; Santa Cruz Biotechnology, USA). The membrane was subsequently processed as described above. Comparison of the expression levels of ZO-1 and Gγ13 in postnatal and adult mice was carried out by collecting olfactory epithelia from 6 P0, 3 P30, and 15 adult animals, pooling the samples from the animals of the same age and preparing tissue lysates as described above. 75, 100, and 130 μg of each extract were separated on a 4–12% Bis-Tris PAGE gel and transferred onto hybond-P. Each membranes which contained samples from either P0 and adult or P30 and adult animals were immunoblotted with a rabbit polyclonal anti ZO-1 mid (1/500; 40–2200; Invitrogen, USA) or a mix of goat polyclonal anti-Gγ13 (1/200 sc-26781 + sc-26782; Santa Cruz Biotechnology, USA) and immunoreactivity evaluated by densitometry (ImageLab; Biorad, USA). The signal intensity for each protein load was expressed as the percentage of the younger animal to the adult and the median value determined.

## IMMUNOHISTOCHEMISTRY

Immunostaining of taste tissue: C57Bl/6J mice deeply anesthetized by intraperitoneal injections of sodium pentobarbital (60 mg/kg) were perfused with 4% paraformaldehyde (PFA). Following perfusion the tongue was removed and circumvallate papillae were excised and soaked 2 h in 4% PFA at 4°C before soaking overnight in 20% sucrose at 4°C. The next day the tissue was snap frozen in isopentane chilled with liquid nitrogen and embedded in OCT medium (Tissue-Tek, Japan) before performing sections (16 μm) on a Leica CM3050S cryostat (Leica Microsystems, Germany). Sections were air dried for 2 h at room temperature, and stored at –80°C. The day of

experiment sections were rehydrated in 0.1 M phosphate saline buffer (PBS, pH 7.4) for 10 min and blocked in 5% goat serum, 0.2% Triton X-100 in PBS for 30 min at room temperature before overnight incubation at 4°C with a 1/100 dilution of the appropriate primary antibodies. Commercial antibodies used were: an affinity purified goat polyclonal anti-G $\gamma$ 13 (sc-26781; Santa Cruz Biotechnology, USA). This antibody was raised against an N-terminal peptide of human G $\gamma$ 13 and has been validated previously on mouse taste tissue (Ohtubo and Yoshii, 2011). Immunoblotting shows that it recognizes G $\gamma$ 13 and does not cross-react with ZO-1 in HEK 293 cells co-expressing both proteins (not shown). A mouse monoclonal anti- $\beta$ -actin (A5441; Sigma, USA), these ascites recognize a single protein of the expected molecular weight in immunoblotting applications (see **Figure 2**). This antibody has been previously used to stain taste buds in rodents (Hofer and Drenckhahn, 1999). An affinity purified rabbit polyclonal anti-GOPC (SAB3500332; Sigma, USA) raised against a 16 amino acid peptide from near the carboxy terminus of human PIST. The specificity of this antibody was tested by the manufacturer. The specificity of this antibody and its restricted staining pattern in mouse taste buds was previously reported (Michlig et al., 2007). A rat monoclonal anti-ZO-1 (MAB1520; Chemicon International, USA). Two rabbit polyclonal anti-ZO-1 (Invitrogen, USA) one raised against amino acids 463–1109 of a human recombinant ZO-1 fusion protein (Cat # 61–7300); the other raised against a synthetic peptide of the mid region of human ZO-1 (Cat # 40–2200). The latter two antibodies recognized a ZO-1 myc tagged protein over-expressed in HEK 293T cells by western blot. Furthermore these antibodies did not cross-react with G $\gamma$ 13 (not shown).

The next day sections were washed repeatedly and incubated for 2 h at room temperature with the appropriate combination of labeled secondary antibodies (1/500 dilution of Alexa 564-conjugated donkey anti-goat IgG (Molecular Probes, USA), 1/500 dilution of Alexa-488-conjugated donkey anti-rabbit IgG (Molecular Probes, USA). Staining specificity was assessed by treating slices in the absence of primary antibodies. After washing and counterstaining with Hoechst 33342 reagent (Sigma, USA), slides were mounted in gel/mount (Biomedica Corp., USA) and analyzed under a TCS-SP2 confocal microscope (Leica, Germany).

Immunostaining of the olfactory epithelium (OE): C57Bl/6J mice were deeply anesthetized by injection of ketamine HCl and xylazine (150 mg/kg and 15 mg/kg body weight, respectively) and then decapitated. The nasal septum was dissected out, the OE removed and subsequently immersed in cold oxygenated ACSF containing in mM: NaCl, 124; CaCl<sub>2</sub> 2; NaH<sub>2</sub>PO<sub>4</sub> 1.25; MgSO<sub>4</sub> 1.3; glucose 15, and NaHCO<sub>3</sub> 26, respectively. Mice olfactory epithelia were then fixed using PFA 4% in PBS containing 0.2% glutaraldehyde. Epithelia were further dipped in 95% ethanol for 1 min, washed three times with PBS, blocked with 2% donkey serum, 2% BSA, and 0.25% Triton X-100 in PBS for 1 h and incubated overnight at 4°C with the primary antibodies diluted in blocking solution. Primary rabbit anti-ZO-1 and goat anti-G $\gamma$ 13 (Santa-Cruz SC-26781) were used at 1:100. Sections were washed three times in PBS and incubated with the secondary antibodies (1:500, goat Alexa488-anti-rabbit, donkey

Alexa488 anti-goat or donkey Alexa555 anti-rabbit, Molecular Probes, Invitrogen) in blocking solution for 2 h at room temperature. Epithelia were mounted between slide and coverslip using MOWIOL 4-88 (Merck, Germany). All Chemicals were from Sigma unless stated.

Samples were visualized using a Leica SP2 laser scanning confocal microscope and a 63 $\times$  oil immersion objective. Ciliary length was used as an indicator of neuron maturity (see Schwarzenbacher et al., 2005) and for each knob the lengths of all the cilia were averaged. Results are given as mean  $\pm$  SEM,  $n$  = number of olfactory knobs.

#### RT-PCR

To analyze the expression of the PDZ domain-containing genes in various tissues 6-weeks-old C57Bl/6J mice were killed with an overdose of sodium pentobarbital, and circumvallate papillae, whole olfactory epithelia (including nasal respiratory epithelium), tongue epithelium devoid of taste buds, liver, and whole brain were dissected out of the carcass on ice. Total RNA extraction, cDNA synthesis and PCR amplification were performed as previously described (Fenech et al., 2009). Primer pairs sequences and annealing temperature are listed in **Table A1**.

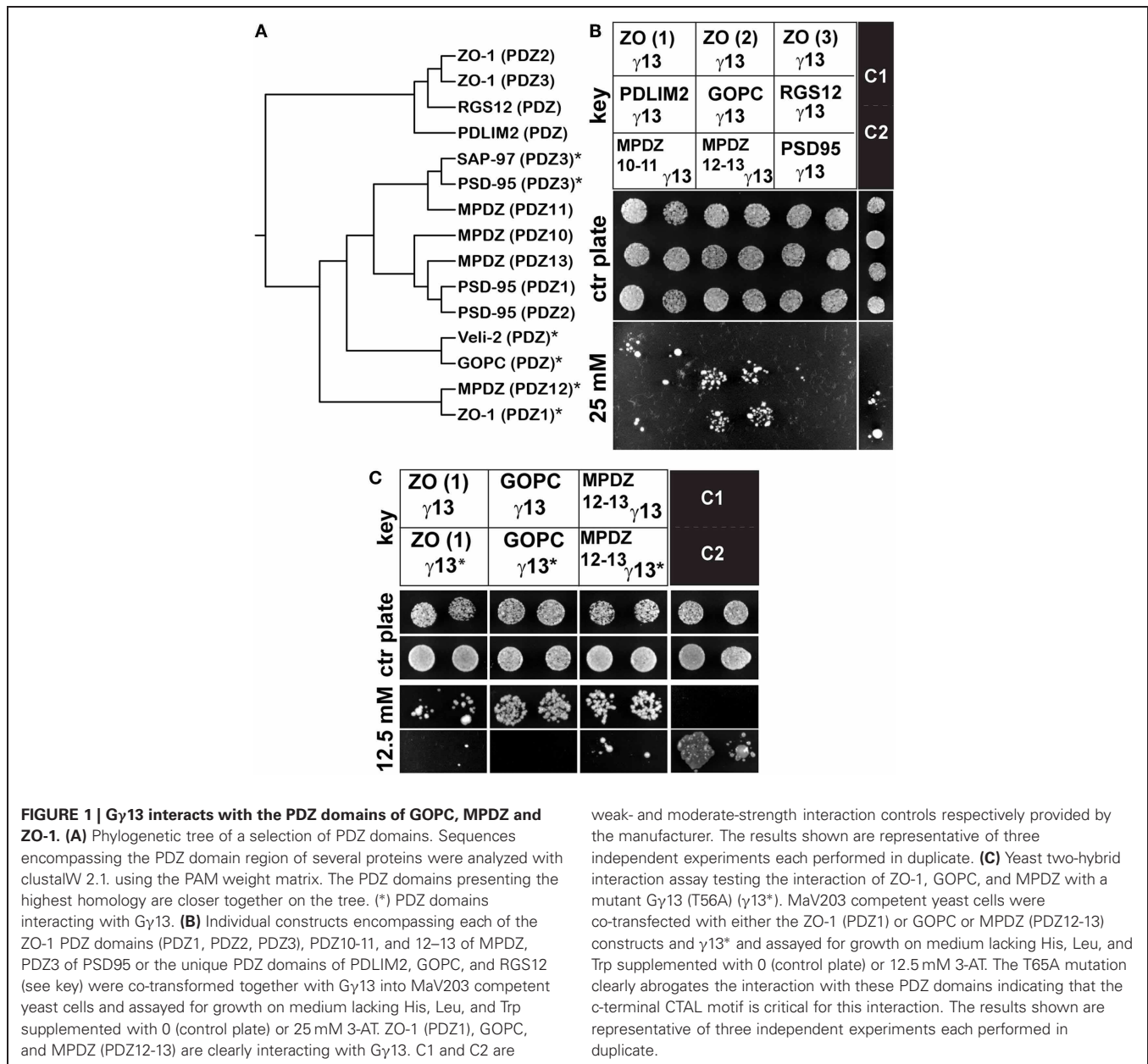
## RESULTS

### G $\gamma$ 13 PHYSICALLY INTERACTS WITH ZO-1, GOPC, AND MPDZ

Earlier work reported an interaction between the C-terminus PDZ binding CTIL motif of G $\gamma$ 13 and the third PDZ domains (PDZ3) of PSD95 or SAP97, or the single PDZ domain of Veli-2 (Li et al., 2006).

To identify additional PDZ-domain containing proteins interacting with G $\gamma$ 13 which might be relevant to taste biology, we conducted a yeast two-hybrid assay using G $\gamma$ 13 as a bait against a selection of five PDZ-domains (Kalyoncu et al., 2010). Some PDZ domains were chosen on the basis of their relative homology to the PDZ3 of PSD95, such as for the multiple PDZ domain protein (MPDZ) PDZ10 and PDZ11 (**Figure 1A**). We also selected the PDZ domains of GOPC (golgi-associated PDZ- and coiled-coil motif-containing protein) and MPDZ PDZ12 which are related to that of Veli-2. In addition, to broadly screen for a novel interaction we also included more divergent PDZ domains such as those of RGS12 (regulator of G protein signaling 12), MPDZ PDZ13, and PDLIM2 (PDZ and Lim domain protein 2). Finally, the three PDZ domains of ZO-1, a tight junction protein belonging to the MAGUK protein family, were also incorporated. MAGUK proteins typically contain multiple PDZ domains and a GUK domain; PSD95 and SAP97 belong to that family.

Plasmids containing either the entire coding sequence of the mouse G $\gamma$ 13 (pBait) or each of the PDZ domain sequences listed above (pPrey) were co-transformed into competent yeast cells and plated out on selective growth media. During an initial screen we uncovered robust interactions with the PDZ1 of ZO-1, the PDZ domain of GOPC and the PDZ12-13 of MPDZ. In contrast, the PDZ domains of RGS12, PDLIM2, PDZ2, and 3 of ZO-1 as well as PDZ10-11 of MPDZ showed weak or no interaction under those conditions (**Figure 1B** and **Table A2**). Note that the PDZ3 of PSD95 which we used as a positive control displayed a relatively weak interaction under these conditions.



It was previously reported that the PDZ binding domain of G $\gamma$ 13 is selective for some but not all PDZ domains within the multi-PDZ domain proteins PSD95 and SAP97 (Li et al., 2006). Our results extend this observation to two additional multi-PDZ domain proteins, namely ZO-1 and MPDZ as well as to the mono-PDZ domain protein GOPC. In the case of ZO-1, the first PDZ domain showed the strongest interaction with G $\gamma$ 13, the second PDZ domain interacted very weakly while the third did not interact at all under our experimental conditions. The interaction with MPDZ was also selective for certain PDZ domains since G $\gamma$ 13 appeared more tightly bound to PDZ12-13 than to PDZ10-11 (Figure 1B). When relating these results to the sequence conservation between these PDZ domains (Figure 1A) it appears that the PDZ

domains most similar to Veli-2 such as GOPC and MPDZ (PDZ12) show a strong affinity for G $\gamma$ 13 whereas the divergent RGS12, PDLIM2, and ZO-1 (PDZ2) are very weak interactors.

#### G $\gamma$ 13 INTERACTS WITH ZO-1 PDZ1 THROUGH A CLASSIC PDZ BINDING MOTIF—PDZ DOMAIN INTERACTION

It is well known that the residue in position -2 in the canonical X(S/T)XA PDZ binding motif, where X is any amino acid and A any hydrophobic amino acid, is critical for the interaction with type I PDZ domains (Bezprozvanny and Maximov, 2001). To confirm the importance of the CTIL motif of G $\gamma$ 13 in the interaction with ZO-1 PDZ1, GOPC, and MPDZ PDZ12-13 we substituted the threonine in position -2 with

an alanine and subsequently tested the ability of the resulting G $\gamma$ 13T65A mutant to interact with these PDZ domains in a yeast two-hybrid assay. As shown in **Figure 1C** and as predicted, the T65A substitution led to a dramatic reduction in the ability of these proteins to interact together. This result supports the notion that G $\gamma$ 13 interacts with these PDZ domains through a classic PDZ binding motif—PDZ domain type interaction (**Table A2**) as previously shown for PSD95 and Veli-2 (Li et al., 2006).

Taken together these results establish for the first time to our knowledge that G $\gamma$ 13 binds selectively to MDPZ PDZ12, GOPC, and ZO-1 PDZ1 via its c-terminal PDZ binding motif.

### EXPRESSION OF G $\gamma$ 13 BINDING PARTNERS

To address whether these newly identified PDZ-containing G $\gamma$ 13 binding partners were expressed in taste tissue and therefore likely to be biologically relevant, we carried out a series of related analyses to look for gene expression and protein content in circumvallate papillae (CV), a site where both G $\gamma$ 13 and bitter taste receptors are abundant (Huang et al., 1999; Matsunami et al., 2000). First we carried out an RT-PCR experiment to look for the expression of the genes coding for GOPC, MPDZ, and ZO-1 in CV, surrounding non-sensory tongue tissue, whole OE, whole brain and liver. Since many splice variants of MPDZ have been reported previously, for this gene we designed primers flanking the 12–13 PDZ domains pair to specifically confirm their expression in CV. In addition, to monitor the presence of OSNs in our OE sample we used specific primers against G $\gamma$ 13 while specific primers against G $\alpha$ gust, a G-protein alpha subunit selectively expressed in a subset of TRCs, allowed us to probe their presence in our CV sample. Glutaraldehyde phosphate dehydrogenase (GAPDH) amplification and a reaction that does not contain reverse transcriptase were carried out as controls to validate the quality of the cDNA reaction and specificity of primer pairs used. Our results show (**Figure 2A**) that ZO-1, GOPC, and MDPZ are broadly expressed and therefore detected in all tissues tested. In contrast G $\gamma$ 13 and G $\alpha$ gust's expression appear restricted to CV and OE samples despite reports of their expression in certain brain cells. We believe that too great of a dilution of the mRNAs for these genes in our whole brain extracts is the reason for the absence of detection in this tissue under our amplification conditions (25 PCR cycles).

To investigate further the localization of the G $\gamma$ 13 interacting proteins in taste bud cells we prepared sections of CV taste buds which were incubated with antibodies raised against MPDZ, GOPC, or ZO-1. Prior to immunohistochemical staining the specificity of the antibodies was verified using immunoblots containing protein extracts from murine CV and OE as well as from HEK 293 cells untransfected or co-transfected with ZO-1 and G $\gamma$ 13 expression constructs. Antibodies raised against MPDZ, GOPC, ZO-1, and G $\gamma$ 13 revealed bands of the expected molecular weight in CV, OE, untransfected and ZO-1/G $\gamma$ 13 transfected HEK 293 cells (**Figure 2B**) thus corroborating the gene expression data obtained by RT-PCR (**Figure 2A**). The presence of additional bands detected by the anti-ZO-1 (in CV, OE, and HEK 293) and anti-MPDZ antibodies in HEK 293 cells is likely linked to the presence of splice variants of these proteins in these cells/tissues.

We noted that the G $\gamma$ 13 protein was of higher molecular weight in CV as compared to OE. Alternative splicing is unlikely to be the reason behind this higher molecular weight since the RT-PCR product generated with primers encompassing the entire coding region of G $\gamma$ 13 is of the expected size in CV and OE (**Figure 2A**). Additional investigations using another antibody directed against an epitope in the middle of the G $\gamma$ 13 coding sequence points toward a post-translational modification preventing binding of the antibody at this site as the higher molecular weight band was not revealed in CV (**Figure A1**). Although, GOPC was detected both in CV and OE it was  $\sim$ 4 fold more abundant in the latter (**Figure 2B**).

Next, we sought to establish whether these proteins were confined to taste bud cells as it is the case for G $\gamma$ 13. Immunostaining of CV sections with the anti-MPDZ antibody revealed the presence of immunopositive taste bud cells (**Figure 2C**). MPDZ was detected mainly in the cytoplasm with a small fraction near the pore.

G $\gamma$ 13 was confined to a subset ( $\sim$ 20%) of taste bud cells, presumably type II cells, and although distributed throughout these cells it was most abundant in the cytoplasm as previously reported. Similarly GOPC was confined to a subset of taste bud cells and its subcellular distribution appeared restricted to the cytoplasm and somewhat near the peripheral plasma membrane (**Figure 2C**).

In contrast, immunostaining with the antibody raised against ZO-1 pointed to a different sub-cellular distribution with most of the protein localized at the taste pore (**Figure 2C**). This distribution is consistent with the location of tight junctions in these cells.

Because of the proximal location of ZO-1 to the microvilli where G $\gamma$ 13 is thought to operate downstream of T2Rs and its role in paracellular permeability paramount to taste cell function, we decided to focus subsequent experiments on the study of the interaction between G $\gamma$ 13 and ZO-1.

### SELECTIVITY AND STRENGTH OF THE INTERACTION BETWEEN G $\gamma$ 13 AND ZO-1

In the next set of experiments, we sought to examine the strength of the interaction between G $\gamma$ 13 with ZO-1 in a more quantitative way. To this end we took advantage of the fact that with the ProQuest yeast two-hybrid system the level of expression of the HIS3 reporter gene is directly proportional to the strength of the interaction between the two assayed proteins. To grade the strength of the interaction between the proteins tested, yeast clones were plated on selection plates lacking histidine and containing increasing concentrations of 3-AT, an HIS3 inhibitor. Yeast clones containing G $\gamma$ 13 and ZO-1 (PDZ1-2) grew on selection plates containing up to 50 mM of 3-AT (**Figure 3A**). This clearly demonstrates a strong interaction between these proteins. The strength of this interaction is only slightly less robust than that observed with claudin-8 a four-transmembrane domain protein integral to taste bud tight junctions previously reported to interact with the PDZ1 of ZO-1 via its c-terminal PDZ binding domain (Itoh et al., 1999; Michlig et al., 2007). No interaction was observed between claudin-8 and ZO-1 (PDZ2-3) as expected; however, G $\gamma$ 13 associated weakly with ZO-1 (PDZ2-3)

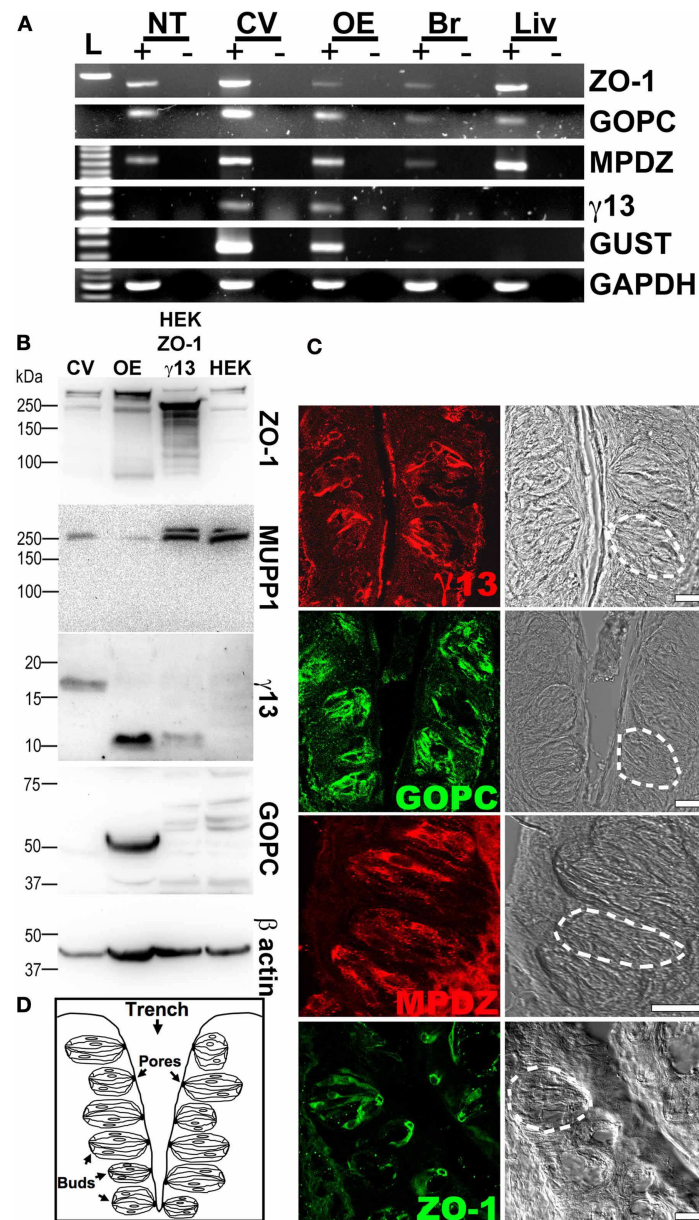


**FIGURE 2 | Expression of GOPC, MPDZ, ZO-1 and Gy13 in circumvallate papillae.** (A) RT-PCR experiment demonstrating expression of ZO-1, GOPC, and MPDZ in all tissues tested. In contrast, the presence of Gy13 and Gγgust (GUST) mRNAs appear to be restricted to taste and olfactory sensory tissues. See Section “RT-PCR” and **Table A1** for details about amplification conditions and expected sizes of PCR products. GAPDH primers were used as a control of the quality of the RNA. (+) and (–) indicate the presence or absence of reverse transcriptase in the reaction respectively. L: 100bp ladder. NT, tongue epithelium deprived of taste buds; CV, circumvallate papillae; OE, olfactory epithelium; Br, whole brain; Liv, liver. The results presented are representative of three independent experiments. (B) Immunodetection of ZO-1, MPDZ, GOPC, and Gy13 proteins in circumvallate (CV) and whole olfactory epithelium (OE) protein extracts. Sample preparation and immunodetection conditions following western blotting are as described in detail under Section “Co-immunoprecipitation and Western blotting.” Protein extracts from HEK 293 cells (HEK) or HEK 293 cells stably expressing HA-Gy13 transiently transfected with a full length Myc-ZO-1 construct (HEK ZO-1 γ13) were used as controls. As expected ZO-1 and Gy13 are detected in CV and OE. Note that Gy13 displays a higher apparent molecular

weight in CV than in OE. Predicted molecular masses for ZO-1, MPDZ, GOPC, Gy13, and β-actin are 220, 220, 51, 8, and 42 kDa respectively. β-actin was used as loading control. The results presented are representative of three independent experiments. (C) Localization of MPDZ, GOPC, Gy13, and ZO-1 proteins in circumvallate taste buds sections. Indirect immunofluorescence on longitudinal cryosections of circumvallate papillae was performed as described under Section “Immunohistochemistry.” MPDZ, GOPC, and Gy13 are mainly distributed in the cytoplasm of a subset of taste bud cells while ZO-1 localizes mostly at the taste pore. On the Nomarski image a white dashed line highlights the size and location of one taste bud. Gy13, MPDZ, and GOPC images are strict confocal optical sections (pinhole 82 μm, airy disk 1) while a wider pinhole was used for the ZO-1 image (pinhole 124 μm, airy disk 1.7). Scale bar = 50 μm. Staining patterns are representative of two independent experiments performed on multiple sections from at least two mice. (D) Drawing representing a longitudinal section of the circumvallate papillae as in (C), showing the location of the taste buds along the walls of the trench under the surface of the tongue. Taste bud cells protrude into the trench through the taste pore.

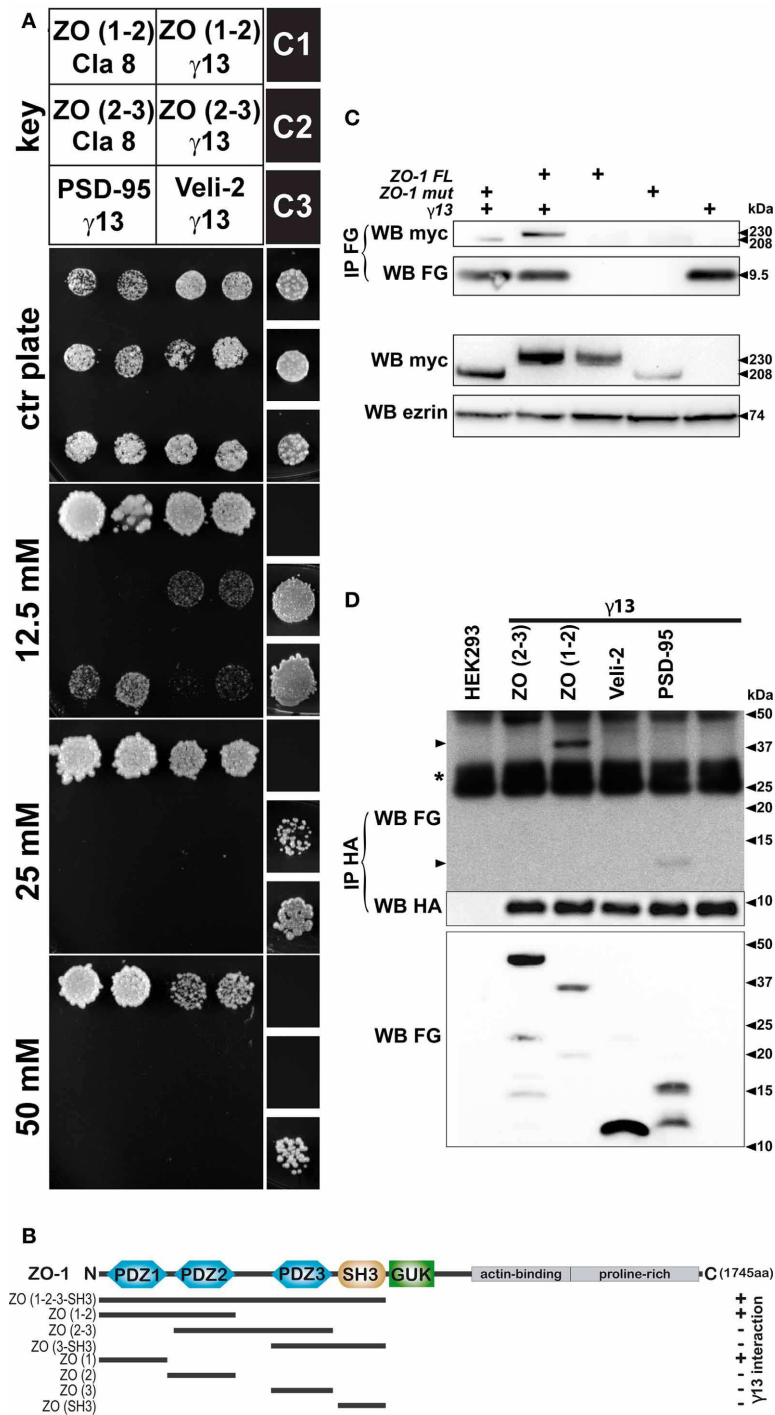


**FIGURE 3 | Physical interaction between heterologously expressed Gy13 and ZO-1. (A)** To test the strength of the interaction between the proteins assayed Mav203 yeasts cells were co-transformed with different combinations of bait and prey plasmids (see key). Interaction was scored on minimal medium plates lacking His, Leu, and Trp but containing increasing concentrations of 3-AT (0–50 mM) a competitive inhibitor of the enzyme involved in histidine biosynthesis. Titration of the strength of the interaction is established by growth potential and compared to weak (C1), moderate (C2) and strong (C3) interaction controls provided by the manufacturer. The construct encompassing the first 2 PDZ domains of ZO-1 [ZO (1–2)] interacts with Gy13 ( $\gamma$ 13) to a similar extent as with the c-terminal tail of claudin 8

(Cla 8) a transmembrane cell–cell interaction protein integral to tight junctions. Weaker interactions between Gy13 and the PDZ2-3 of ZO-1 [ZO (2–3)], the PDZ3 of PSD95 (PSD95), or the unique PDZ domain of Veli-2 (Veli-2) were also observed. Note that no interaction between claudin 8 and ZO (2–3) was visible as expected. The results presented are representative of three independent experiments performed in duplicate. **(B)** Schematic drawing recapitulating the different domains of ZO-1 tested for their interaction with Gy13 by two-hybrid interaction assay. At the top simplified representation of the organization of protein domains in ZO-1 showing the PDZ1, PDZ2, PDZ3, SH3, GUK, actin-binding and proline-rich

(Continued)

**FIGURE 3 | Continued**

domains. The span of the constructs tested by two-hybrid are shown underneath (black line). The ability of the ZO-1 constructs to interact with G $\gamma$ 13 in presence of 25 mM 3-AT were scored with a (+) when growth was observed or (–) when there was no growth. An interaction with G $\gamma$ 13 was detected whenever the construct contained the first PDZ domain of ZO-1. **(C)** To ensure that G $\gamma$ 13 could interact with the native ZO-1 protein, expression constructs encoding tagged full length ZO-1, or G $\gamma$ 13 proteins were transiently transfected into HEK 293 cells. Protein extracts were prepared from cells expressing full length MYC-ZO-1 (ZO-1FL, lane 3), MYC-ZO-1 missing the PDZ1 domain (ZO-1mut, lane 4), FLAG-G $\gamma$ 13 (lane 5) or co-expressing FLAG-G $\gamma$ 13 and MYC-ZO-1FL (lane 2), or FLAG-G $\gamma$ 13 and MYC-ZO-1mut (lane 1) as indicated. Examination of the expression of MYC-ZO-1 and MYC-ZO-1mut expression by western blot with anti-MYC (WB myc, second to last panel) revealed that both proteins are produced (~230 and ~208 kDa respectively). Erzin was used as a loading control (WB erzin). Protein extracts were used to immunoprecipitate the FLAG-G $\gamma$ 13 protein with an anti-FLAG antibody (IP FG, WB FG). Analysis of the content of the immunoprecipitated complex (IP FG) using an anti-myc antibody (WB myc) confirms the interaction of the ZO-1FL or ZO-1mut proteins with G $\gamma$ 13 in the

samples co-expressing ZO-1FL or ZO-1mut and FLAG-G $\gamma$ 13 (lane 1 and 2). Two additional experiments yielded the same results. **(D)** To validate the interactions uncovered using the yeast two-hybrid interaction assay and in particular the protein domains of ZO-1 important for the interaction with G $\gamma$ 13, co-immunoprecipitation experiments were performed in HEK 293 cells following heterologous co-expression of HA-G $\gamma$ 13 with various FLAG-ZO-1 deletion constructs. Cells were left untransfected (lane 1) or transiently transfected with HA-G $\gamma$ 13 alone (lane 6) or in combination with FLAG-ZO-1(PDZ2-3) (lane 2), FLAG-ZO-1(PDZ1-2) (lane 3), FLAG-Veli-2(PDZ) (lane 4), or FLAG-PSD95(PDZ3) (lane 5) as indicated. Protein extracts from transfected cells were first analyzed for expression of the FLAG-tagged deletion constructs by western blot using an anti-FLAG antibody (WB FG, bottom panel). Then anti-HA immunoprecipitation was carried out and complexes were analyzed by western blot using an anti-FLAG antibody (IP HA, WB FG, top panel). FLAG-PSD95 and FLAG-ZO-1(PDZ1-2) are detected (arrowheads) indicating that these domains interact with G $\gamma$ 13 under these conditions. Anti-HA western analysis of the samples confirms correct immunoprecipitation of HA-G $\gamma$ 13 (IP HA, WB HA, middle panel). (\*) IgG light chains. The experiment shown is representative of 3 independent experiments.

presumably through a direct interaction with the second PDZ domain of ZO-1 (see **Figure 1B**).

**INTERACTION OF G $\gamma$ 13 AND ZO-1 IN HEK 293T CELLS**

To validate our yeast two-hybrid assay interaction results between ZO-1 and G $\gamma$ 13 we next tested whether these proteins would co-immunoprecipitate when co-expressed in HEK 293 cells. In order to rule out the possibility that folding of the native protein would prevent this interaction, full-length ZO-1 and G $\gamma$ 13 constructs were used for this experiment. HEK 293 cell lines stably expressing a MYC-ZO-1 or a MYC-ZO-1 mutant lacking the PDZ1 domain (generous gift of A. Fanning) (Fanning et al., 1998) were transiently transfected with a FLAG-G $\gamma$ 13 (generous gift of B. Malnic) (Kerr et al., 2008) construct. Forty-eight hours later protein extracts from these cells were prepared and used for immunoprecipitation using an anti-FLAG antibody. Western blot analysis of simple protein extracts from transfected cells using anti-MYC and anti-FLAG antibodies confirms that all full length and mutant proteins are produced in these cells (**Figure 3B**). Immunoprecipitation of G $\gamma$ 13 using an anti-FLAG antibody pulled down both intact MYC-ZO-1 and mutant constructs thus supporting further our contention that G $\gamma$ 13 and ZO-1 physically interact. The interaction of the MYC-ZO-1 mutant construct with G $\gamma$ 13 despite the absence of the PDZ1 domain can potentially be explained by the fact that as shown in **Figures 1B** and **3A** G $\gamma$ 13 interacts weakly with the PDZ2 of ZO-1 in yeast cells. Alternatively, it is possible that the transfected MYC-ZO-1 mutant binds the endogenous ZO-1 (see **Figure 2B**) through an already documented PDZ2 mediated interaction (Uteperbergenov et al., 2006). This homodimer would allow G $\gamma$ 13 to be pulled down along with the MYC-ZO-1 mutant through an interaction with the ZO-1 PDZ1 of the endogenous ZO-1.

In order to further investigate these two possibilities we generated two truncated FLAG-tagged ZO-1 constructs encompassing either the first and second (PDZ1-2) or the second and third (PDZ2-3) PDZ domains of ZO-1 as well as a G $\gamma$ 13 construct

harboring an HA tag at the N-terminal. We also made FLAG-PSD95 (PDZ3), and FLAG-Veli-2 (PDZ) control constructs. The HA-G $\gamma$ 13, along with each FLAG-tagged construct were transfected in HEK 293 cells. Forty-eight hours after transfection the cell lysates were subjected to immunoprecipitation with an anti-HA antibody. Lysates from untransfected cells and cells transfected with the HA-G $\gamma$ 13 construct alone were used as controls. Analysis of the immunoprecipitates by immunoblotting using an anti-FLAG antibody showed that G $\gamma$ 13 co-precipitated with ZO-1 (PDZ1-2) and PSD95 (PDZ3) but not with ZO-1 (PDZ2-3) or Veli-2 (PDZ) (**Figure 3C**). Analysis of the HEK 293 cell lysates by immunoblot using an anti-FLAG antibody indicates that all the FLAG-tagged constructs including ZO-1 (PDZ2-3) and Veli-2 (PDZ) were produced and therefore available for co-immunoprecipitation. These results corroborate our yeast two-hybrid assay results (**Figures 1B** and **3A**) and effectively rule out the possibility that binding of G $\gamma$ 13 to the second PDZ domain of ZO-1 is strong enough to withstand the harsh conditions of this assay. We also note that under these conditions the weak interaction between G $\gamma$ 13 and Veli-2 is not recapitulated.

Yeast two-hybrid and co-immunoprecipitation assay data strongly supporting a direct interaction between the c-terminal 4 amino-acids of G $\gamma$ 13 and the first PDZ domain of ZO-1 are recapitulated in **Figure 3D**.

**PARTIAL CO-LOCALIZATION OF MPDZ, GOPC, OR ZO-1 WITH G $\gamma$ 13 IN MOUSE TASTE BUD CELLS**

In circumvallate taste buds G $\gamma$ 13's expression is restricted to type II cells where it is thought to play a role in bitter taste signal transduction (Huang et al., 1999; Clapp et al., 2001). In addition, immunohistochemical analysis of circumvallate, fungiform or soft palate papillae indicates that G $\gamma$ 13 is particularly abundant in the cytoplasm of these cells (Clapp et al., 2001; Ohtubo and Yoshii, 2011). To test whether MPDZ, GOPC, and ZO-1 are co-localized with G $\gamma$ 13 in mouse taste bud cells, circumvallate papillae were dissected out and double-immunofluorescent labeling experiments on sagittal cryosections were performed.

Optical sections of tissue were acquired under a confocal microscope focusing on the region of interest and overlaid with the software.

Analysis of tissue sections co-stained with G $\gamma$ 13 (**Figure 4A**) and MPDZ (**Figure 4C**) focusing on confocal optical sections near the pore shows that a small fraction of the G $\gamma$ 13 staining overlaps with that of MPDZ in that area (**Figure 4B**). On tissue sections double labeled with GOPC (**Figure 4D**) and G $\gamma$ 13 (**Figure 4E**) analysis of single optical sections through the cytoplasm of taste bud cells where G $\gamma$ 13 is abundant, revealed an extensive co-localization with GOPC at that location (**Figure 4E**). In addition, a similar partial co-localization pattern between ZO-1 (**Figure 4G**) and G $\gamma$ 13 (**Figure 4I**) was observed on single optical sections through the taste pore (**Figure 4H**). This pattern was further confirmed using two additional antibodies raised in a different host and targeting different epitopes in ZO-1 (data not shown). Partial co-localization between MPDZ, GOPC, or ZO-1, and G $\gamma$ 13 in taste bud cells indicates that these proteins might be involved in a dynamic process within the cell and supports the claim that they are likely biological partners.

These experiments also revealed that all TRCs expressing G $\gamma$ 13 are immunopositive for GOPC, further emphasizing a tight collaboration between these two proteins. GOPC immunoreactivity was observed as well in cells that did not express G $\gamma$ 13 (**Figure 4E**), presumably in type I or III cells. Unfortunately the rather weak immunostaining with the MPDZ specific antibody and the very restricted location of ZO-1 around the tight junctions prevented an in depth study of the cell types expressing these proteins.

#### CO-LOCALIZATION OF ZO-1 AND G $\gamma$ 13 IN OLFACTORY SENSORY NEURONS

Both ZO-1 and G $\gamma$ 13 have been independently reported to be expressed in OSNs (Miragall et al., 1994; Kulaga et al., 2004). In order to investigate whether G $\gamma$ 13 and ZO-1 co-localize in olfactory neurons, we set-up a flat-mount (or « en face ») preparation of OE allowing us to image individual olfactory neuron dendritic knobs. First, in P30 mice no co-localization between G $\gamma$ 13 and ZO-1 was ever seen in G $\gamma$ 13 immunopositive knobs ( $n = 220$ , **Figure 5A**). Next, we analyzed newborn mice (P0). At this stage dendritic knobs could be split into two groups (Schwarzenbacher et al., 2005). A first group did not display any cilia and was recognizable by its round smooth aspect (**Figure 5B**). In this group co-localization was found in 66.6% of the dendritic knobs ( $n = 9$  knobs). In a second more important group encompassing dendritic knobs bearing small ciliary compartments (**Figure 5C**) co-localization between G $\gamma$ 13 and ZO-1 was seen in 73% of the ciliated dendritic knobs ( $n = 27$  knobs). Overall co-localization could be observed in 72.2% of the G $\gamma$ 13 immunopositive dendritic knobs ( $n = 36$ ) at P0. Finally and in line with these observations, dendritic knobs where co-localization between the two proteins was seen had shorter cilia (average length per knobs  $2.8 \pm 0.2$  mm,  $n = 20$ ) compared to the ones where no co-localization was observed ( $n = 5.5 \pm 1.0$  mm,  $n = 7$ ,  $p < 0.01$  Mann-Whitney). We, therefore, infer that co-localization between G $\gamma$ 13 and ZO-1 depends upon the developmental stage of olfactory neurons. Note that

the secondary antibody alone did not produce any background staining (**Figure 5D**).

Next ZO-1 and G $\gamma$ 13's protein expression levels in olfactory mucosa were evaluated during development by western blot. The signal intensity expressed as the percentage of the younger animal to the adult indicates that there is a slight decrease of ZO-1 expression from 84% at P0 to 63% at P30 while G $\gamma$ 13's expression increased from 15% at P0 to 33% at P30. Given these results we cannot completely rule out the possibility that the lack of co-localization observed at P30 might be linked with the slight decrease of ZO-1 expression at this stage.

## DISCUSSION

### A NETWORK OF PROTEINS POTENTIALLY REGULATING THE INTRACELLULAR TRAFFIC OF G $\gamma$ 13 IN TASTE RECEPTOR CELLS

Following up on an earlier report demonstrating an interaction between G $\gamma$ 13 and the PDZ domain containing proteins Veli-2 and SAP97, our data identified GOPC, MPDZ, and ZO-1 as binding partners of G $\gamma$ 13. We also report for the first time to our knowledge the expression of GOPC and MPDZ in taste bud cells.

All three PDZ-containing proteins identified in this study are known members of macromolecular complexes or participate in protein trafficking suggesting that they are likely to determine G $\gamma$ 13's transport and/or subcellular location in taste cells.

GOPC is a Golgi-associated protein reportedly interacting with a number of transmembrane proteins including channels and GPCRs for which it is thought to modulate vesicular transport from the Golgi apparatus to the plasma membrane. In addition it is known to associate with the Rho effector Rhotekin at adherent junctions where it is thought to regulate cell-polarity development (Ito et al., 2006). These features might explain in part both the punctate staining pattern as well as the staining observed at the periphery of the taste bud cells (**Figure 2C**). Although, this is the first report of GOPC's expression in TRCs, this new finding is not totally surprising considering that TRCs are polarized neuroepithelial sensory cells much like inner ear sensory hair cells of the cochlea where GOPC regulates membrane trafficking of cadherin 23 (Xu et al., 2010), a cell-cell adhesion protein also found in retinal cells where its loss is associated with retinitis pigmentosa (Bolz et al., 2001). In hair cells GOPC retains cadherin 23 in trans-golgi networks (TGNs). Co-expression of MAGI-I and harmonin, two PDZ domain-containing proteins, competes with GOPC to cause the release of cadherin 23 from the TGN. It is plausible that in TRCs MPDZ, which we find distributed in the cytoplasm and to a small extent near the tight junctions, fulfills the same function as MAGI-I. Under this scenario we would assume that MPDZ is able to compete with GOPC for G $\gamma$ 13 binding and once unloaded onto MPDZ, G $\gamma$ 13 is transported to the taste bud pore. Coincidentally, MPDZ has been reported to interact with the tight junction complex, particularly with claudin-1 in polarized epithelial cells; therefore, its localization at the pore is not completely unexpected (Hamazaki et al., 2002; Liew et al., 2009). Our own experiments corroborate these findings by showing that although MPDZ seems most abundant in the cytoplasm of taste bud cells, a fraction of it is detected at the pore where it is partly co-localized with ZO-1 (**Figure A2**).

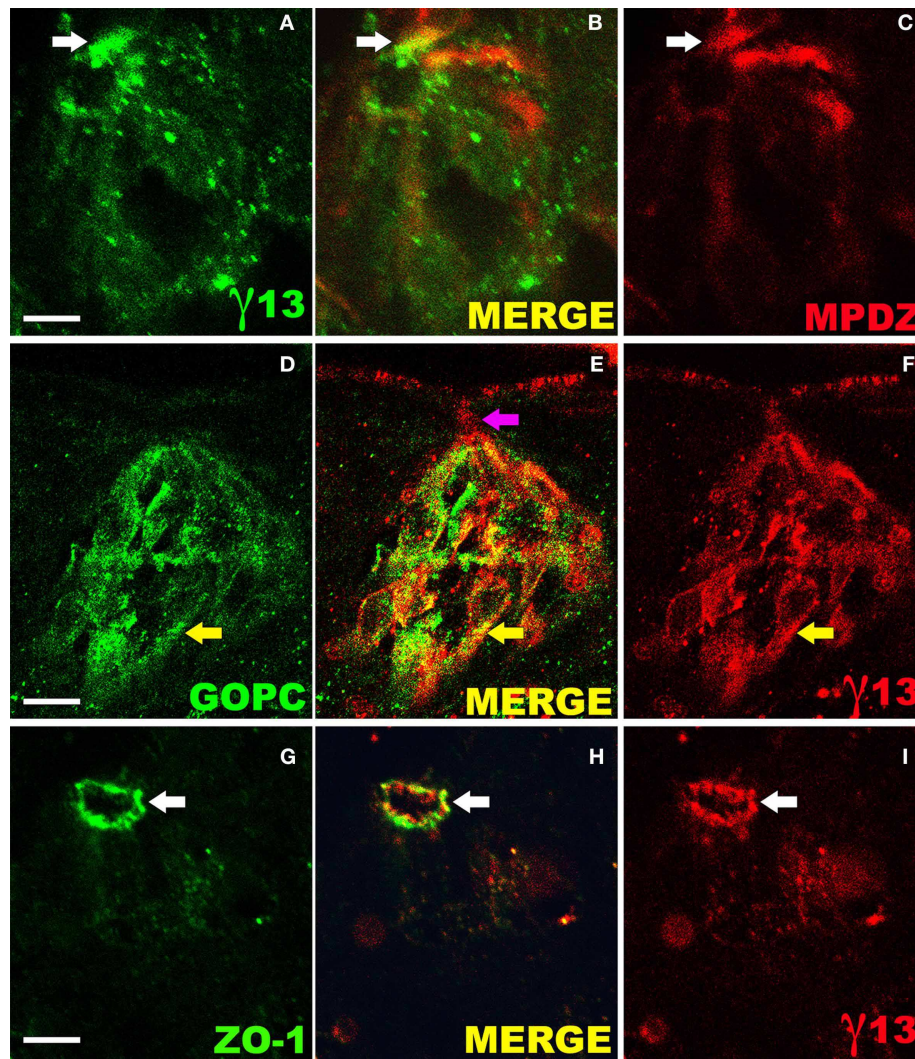


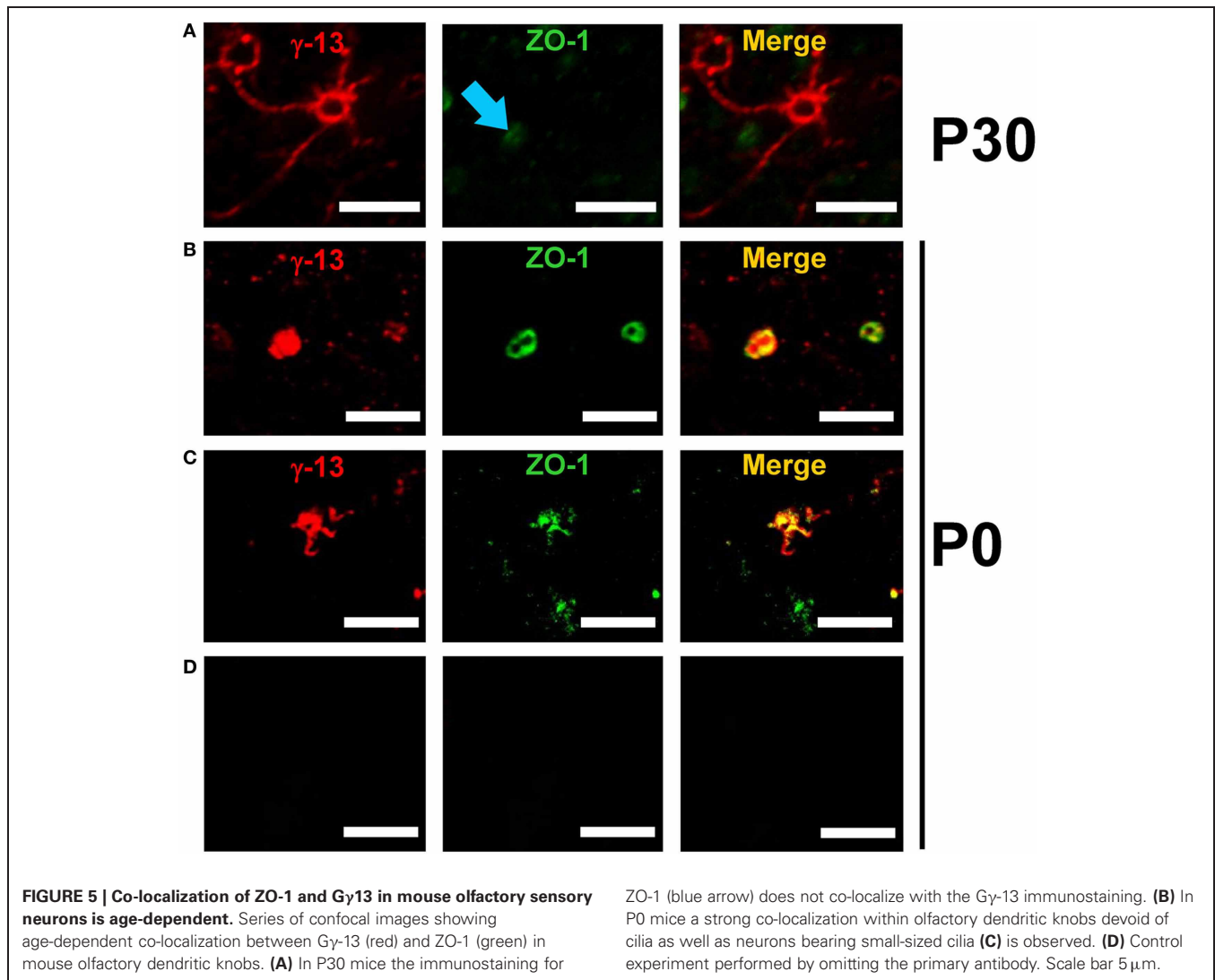
**FIGURE 4 | Partial co-localization of G $\gamma$ 13 with its interaction partners in mouse taste bud cells.** Laser scanning confocal microscope analysis of sagittal sections of circumvallate papillae incubated simultaneously with specific antibodies raised against G $\gamma$ 13 and either ZO-1, MPDZ, or GOPC and revealed with the appropriate fluorescent secondary antibodies. Each image shows one entire taste bud (apical: up, basal: down). Partial co-localization between G $\gamma$ -13 and MPDZ (**A–C**) is observed in the cytoplasm and to a small extent the pore (white arrows). GOPC and G $\gamma$ -13 staining (**D–F**) shows an

extensive overlap in the cytoplasmic region (yellow arrows) but not near the pore (purple arrow). Partial co-localization of ZO-1 and G $\gamma$ -13 (**G–I**) is evident at the pore where tight junctions are located. The images presented are single optical sections (not stacks) collected under strict confocal conditions (airy disk 1, GOPC/G $\gamma$ -13 Pinhole 82  $\mu$ m, GOPC or ZO-1/G $\gamma$ -13 Pinhole 115  $\mu$ m). Confocal images were merged electronically using Photoshop. Scale bar 15  $\mu$ m. Images are representative of staining patterns obtained in >6 taste buds from three mice.

Alternatively Veli-2, another cytosolic G $\gamma$ 13 binding protein might be able to fulfill the same function (Li et al., 2006). It is interesting to note that both MAGI-I and MDPZ have several (>5) PDZ domains suggesting that in addition to G $\gamma$ 13 they might concomitantly bind additional proteins such as receptors and channels. GABA $\beta$  receptors which have been detected in TBCs and shown to interact with MPDZ represent such an example (Balasubramanian et al., 2007; Cao et al., 2009). Once at the tight junction, ZO-1 would allow docking of G $\gamma$ 13 and perhaps regulate its entry into the microvilli. In this regard, it is worth noting that detection of G $\gamma$ 13 in microvilli of TRCs appears weak compared to what is observed in olfactory cilia suggesting that

entry of G $\gamma$ 13 in microvilli is tightly regulated. Alternatively, this interaction might affect paracellular permeability as discussed below.

It is conceivable that within the microvilli G $\gamma$ 13 could travel to the apical tip through an interaction with the PDZ domain containing protein SAP97 as previously suggested (Li et al., 2006). There G $\gamma$ 13 would become anchored to the plasma membrane following prenylation of its c-terminal cysteine residue. This event would signal the end of the road for G $\gamma$ 13 as prenylation is preceded by the removal of the residues downstream of the cysteine thus eliminating the PDZ binding site as previously noted by Li et al. (2006). At its final destination G $\gamma$ 13 would presumably



assemble with G $\beta$ 1 and G $\alpha$ gust to participate in signaling downstream of T2R receptors (Huang et al., 1999). Although the exact sequence of events remains to be confirmed we note that the short sequence between the  $\beta$ B and  $\beta$ C regions of the PDZ domains of PSD95 and Veli-2 thought to accommodate the prenyl group of G $\gamma$ 13 (Li et al., 2006) is absent from ZO-1 (PDZ1) and MPDZ (PDZ12) (**Figure A3**) perhaps indicating that prenylation occurs later in this sequence.

#### G $\gamma$ 13 AT THE TIGHT JUNCTION

The tight junction of polarized epithelial cells plays a fundamental role in the regulation of the paracellular permeability barrier as well as the maintenance of apical and basolateral compartments. Interestingly, heterotrimeric G protein signaling has been implicated in tight junction biogenesis and permeability regulation. Consistent with this a number of modulators of G protein activity (AlF4, cholera, and pertussis toxins) affect tight junction assembly (Balda et al., 1991) and several G protein  $\alpha$  subunits including G $\alpha$ i2, G $\alpha$ o, G $\alpha$ 12, and G $\alpha$ s have been located at the tight

junction (Saha et al., 2001). In fact, it was recently shown that activation of G $\alpha$ 12, which interacts directly with ZO-1 through its SH3 domain, disrupts the tight junction through a c-Src mediated pathway thereby increasing paracellular permeability (Meyer et al., 2002; Sabath et al., 2008). Heterotrimeric G proteins mediate GPCR signaling through G $\alpha$  and G $\beta$  $\gamma$  subunits and as expected one GPCR has been reported to regulate tight junction permeability in a pertussis-sensitive manner. This is the case of the somatostatin 3 receptor (SSTR3) which is targeted to the tight junction through a direct interaction between a PDZ binding motif in its c-terminal tail and MPDZ PDZ10 (Liew et al., 2009). Finally, another component of the G protein cascade, namely regulator of G protein signaling 5 (RGS5) has also been reported to interact with ZO-1 (Bal et al., 2012).

Although there are no prior reports of G $\beta$  $\gamma$  subunits at the tight junction, our finding that G $\gamma$ 13 interacts directly with ZO-1 and MPDZ is not totally unexpected. However the role it might play on TJ assembly, maintenance of polarity, or paracellular permeability in taste bud cells remains to be established.

### Gy13 IN OLFACTORY SENSORY NEURONS

In stark contrast to what is observed in microvilli, Gy13 is readily detected in cilia of OSNs where it is thought to be involved in sensory signaling. Our observation that Gy13 and ZO-1 co-localize in the OE of neonates but not in that of adult animals suggests that this interaction might be important during the maturation of the epithelium in mice. In adult rat OE, ZO-1 is localized at apical tight junctions connecting the dendrites of OSNs and surrounding supporting cells (Miragall et al., 1994). Claudins 1, 3, 4, and 5 are part of the apical tight junction complex forming a selective barrier necessary for proper signaling in OSNs (Steinke et al., 2008). Despite the fact that tight junctions in TRCs and OSNs share a number of components including claudin 1, claudin 4, and ZO-1, the absence of co-localization between Gy13 and ZO-1 in the adult OE clearly points to important organizational dissimilarities in these tissues.

Another notable difference between these tissues includes the fact that in OSNs MPDZ is mainly restricted to the cilia where it is thought to regulate odorant evoked signal duration through a direct interaction with odorant receptors (Dooley et al., 2009). As a result, MPDZ has been deemed a major component of the signalosome downstream of odorant receptors also known as “olfatosome.” Our findings extend this concept by showing that another component of the olfactory signaling cascade abundant in cilia, namely Gy13, also interacts with MPDZ.

Although, there are no current reports of GOPC in OSNs, here we present data indicating that GOPC is detected in the OE. While its precise location and sub-cellular distribution in the OE remains to be investigated, we suspect that it is involved in retention of Gy13 in the TGN.

### Gy13 AND SENSORY SIGNALING

GPCRs couple selectively to  $G\alpha$  subunits which themselves associate selectively with  $G\beta\gamma$  subunits. Upon stimulation of the receptor, both  $G\alpha$ - and  $G\beta\gamma$ -mediated processes are activated. Determinants effectively governing downstream events include the repertoire of  $G\alpha$ ,  $G\beta$ ,  $G\gamma$  and cellular effectors present in the cells expressing the receptor in question as well as the selectivity of the interactions between receptor and  $G\alpha$  subunits and that between  $G\gamma/G\beta$  subunits and cellular effectors.

If we apply this reasoning to TRCs we note that both  $G\alpha_{\text{gust}}$  and  $G\alpha_{\text{i2}}$  are present (McLaughlin et al., 1992; Kusakabe et al., 2000), and that functional and biochemical studies indicate that T2Rs are able to couple to and activate both  $G\alpha_{\text{i/o}}$  and  $G\alpha_{\text{gust}}$  subunits (Ozeck et al., 2004; Sainz et al., 2007). Experiments with gustducin knock-out (KO) animals implicate both  $G\alpha_{\text{gust}}$  and additional  $G\alpha$  subunits in bitter transduction as the KO mice retained sensitivity to bitter substances (Wong et al., 1996). Regarding the beta and gamma subunits, both  $G\beta_1$  and  $G\beta_3$  have been detected in gustducin expressing cells together with  $G\gamma_3$  and  $G\gamma_{13}$  (Huang et al., 1999; Rossler et al., 2000).

Based on these accounts many possible  $G\alpha$ ,  $G\beta$ ,  $G\gamma$  combinations may mediate bitter detection in mammals. Nevertheless, it is thought that the heterotrimer composed of  $G\alpha_{\text{gust}}/G\beta_3/G\gamma_{13}$  is the main player. Under this scenario the  $G\beta_3$ - $G\gamma_{13}$  complex activates phospholipase C- $\beta_2$  (PLC- $\beta_2$ ) or PLC- $\beta_3$  (Hacker et al., 2008) while  $G\alpha_{\text{gust}}$  acts in parallel on local phosphodiesterases

to modulate intracellular cAMP levels. A recent report puts forward an alternative role for  $G\alpha_{\text{gust}}$  in taste cells by demonstrating that its constitutive activity maintains low resting cAMP levels thereby regulating the responsiveness of bitter receptor cells (Clapp et al., 2008). This new hypothesis does not take away from the demonstrated central role of PLC- $\beta_2$  in bitter transduction (Zhang et al., 2003) and the possible involvement of Gy13 in this process. Nevertheless, a tissue-specific KO model validating the role of Gy13 in bitter taste transduction *in vivo* is still missing.

Unlike in the taste cells where PLC signaling is paramount to GPCR-mediated tastant detection, in OSNs disruption of the cAMP pathway leads to anosmia (Brunet et al., 1996; Belluscio et al., 1998; Wong et al., 2000). In olfactory cilia Gy13 co-localizes and is thought to interact with  $G\beta_1$  and  $G\alpha_{\text{olf}}$  (Kerr et al., 2008). Although, the recombinant  $G\beta_1\gamma_{13}$  dimer appears to be the second most potent activator of PLC- $\beta$  isoforms after  $G\beta_1\gamma_7$  (Poon et al., 2009), the absence of a convincing demonstration of PLC- $\beta$  expression in OSNs suggests that in these cells Gy13 might play another role. Kerr et al. reported that Gy13 interacts with Ric-8B, a guanine nucleotide exchange factor for  $G\alpha_{\text{olf}}$ , and hypothesized that by retaining Ric-8B in proximity of  $G\alpha_{\text{olf}}$ -GTP, Gy13 would facilitate re-association of Ric-8B and  $G\alpha_{\text{olf}}$ -GDP which ultimately would maximize the efficiency of that pathway.

Our immunostaining experiments suggest that Gy13 interacts with ZO-1 temporarily during the maturation of the OSN. The impact this interaction might have on sensory signaling or OSN maturation remains to be investigated. Functional maturation is known to occur in OSNs (Lee et al., 2011). This maturation could be correlated with signaling protein trafficking and involve ZO-1 as it was previously implicated in maturation and regeneration in other cell types (Castillon et al., 2002; Kim et al., 2009). Under this scenario it is conceivable that the interaction between ZO-1 and Gy13 during OSN maturation might induce some functional changes. In this case a tissue-specific Gy13 KO mouse model will be a valuable tool to help unravel the role of this protein in OSN function *in vivo*.

Finally, in mouse cone and rod bipolar cells Gy13 appears to be distributed throughout the cells while  $G\alpha_{\text{o}}$  is concentrated in dendrites. The co-expression of Gy13 with  $G\beta_3$ ,  $G\beta_4$ , and  $G\alpha_{\text{o}}$  in ON cone bipolar cells which do not contain PLC- $\beta$  suggests that it might be involved in yet another signaling pathway in these cells (Huang et al., 2003). In this tissue where ZO-1 expression has been reported as well (Ciolofan et al., 2006), it would be interesting to investigate whether these proteins are partly co-localized.

### CONCLUSION

In the present study, we report the identification of three novel binding partners for Gy13. In addition, we provide the first evidence of the expression of two of these proteins (GOPC and MPDZ) in taste bud cells. We anticipate that future work addressing the sequence of these interactions with Gy13 and their temporality will help shed more light on the precise role these proteins play in efficiently targeting Gy13 to selective subcellular locations.

By comparing the subcellular location of some of these proteins in OSNs and neuroepithelial taste cells, our study points out possible discrepancies in the mechanisms guiding protein traffic

and subcellular localization in these two cell types. These differences might not be surprising given the differences in the origin (neuronal vs. epithelial) and the architecture of neuroepithelial taste cells and OSNs. In particular, we believe that the differential location of MPDZ and Gy13 in OSNs and TRCs reflects different mechanisms at play in both types of sensory cells and provides some clues as to what their function in these cells might be (transport vs. signalosome). Interestingly, MPDZ is thought to act as a scaffolding protein in the spermatozoa, a polarized cell capable of chemotaxis through taste and odorant receptors (Zitanski et al., 2010).

The presence of MPDZ, ZO-1, and Gy13 at the tight junction in TRCs is intriguing and remains to be investigated further. In this context it is interesting to mention that ZO-1 has been demonstrated to associate with F-actin through an actin-binding region located in the C-terminal half of the molecule (Fanning et al., 2002) and that F-actin filaments are major structural components of taste cells microvilli (Takeda et al., 1989).

Finally, we would like to mention that given the expected importance of Gy13 in taste cells signaling, disruption of any of the interactions reported here could have important consequences on taste reception. There is such a precedent in the OE where polymorphisms in CEP290, a protein which cargoes Gy13,

Gαs, and Gβ1 from the base of the cilia toward the tip, have been linked with anosmia (McEwen et al., 2007).

## ACKNOWLEDGMENTS

We would like to thank Dr. A. Fanning (University of North Carolina at Chapel Hill, USA) for providing the Myc-tagged ZO-1 constructs and kindly sharing protocols with us, Dr. O. Keskin (Koç University, Turkey) for help with the classification of PDZ domains, Dr. E. Assémat (IBDML, Marseille) and C. Neophytou (Emergo, Cyprus) for advice on MPDZ and ZO-1 antibodies respectively, Dr. C. Arnould (INRA, Dijon) for help with confocal microscopy and A. Lefranc for help with animal husbandry. We are grateful to Dr. B. Malnic (University of Sao Paulo, Brazil) for the FLAG-Gy13 construct, insightful comments and suggestions throughout, Dr. V. Dionne (Boston University, USA) for critical reading of the manuscript, and Dr. G. Strichartz (Brigham and Women's Hospital, USA) for support. This work was supported by Action Thematique Incitative sur Programme (CNRS) grants to Jean-Pierre Montmayeur and Xavier Grosmaître, Région de Bourgogne and CNRS poste rouge post-doctoral fellowships to Zhenhui Liu and Esmerina Tili respectively, and funds from GOSPEL (IST-2002-507610) to Fabienne Laugerette and Anna Wiencis.

## REFERENCES

- Anderson, J. M., Stevenson, B. R., Jesaitis, L. A., Goodenough, D. A., and Mooseker, M. S. (1988). Characterization of ZO-1, a protein component of the tight junction from mouse liver and Madin-Darby canine kidney cells. *J. Cell Biol.* 106, 1141–1149.
- Balasubramanian, S., Fam, S. R., and Hall, R. A. (2007). GABAB receptor association with the PDZ scaffold Mupp1 alters receptor stability and function. *J. Biol. Chem.* 282, 4162–4171.
- Bal, M. S., Castro, V., Piontek, J., Rueckert, C., Walter, J. K., Shymanets, A., Kurig, B., Haase, H., and Blasig, I. E. (2012). The hinge region of the scaffolding protein of cell contacts, zonula occludens protein 1, regulates interacting with various signaling proteins. *J. Cell. Biochem.* 113, 934–945.
- Balda, M. S., Gonzalez-Mariscal, L., Contreras, R. G., Macias-Silva, M., Torres-Marquez, M. E., Garcia-Sainz, J. A., and Cerejido, M. (1991). Assembly and sealing of tight junctions: possible participation of G-proteins, phospholipase C, protein kinase C and calmodulin. *J. Membr. Biol.* 122, 193–202.
- Belluscio, L., Gold, G. H., Nemes, A., and Axel, R. (1998). Mice deficient in G(olf) are anosmic. *Neuron* 20, 69–81.
- Bezprozvanny, I., and Maximov, A. (2001). Classification of PDZ domains. *FEBS Lett.* 509, 457–462.
- Bolz, H., von Brederlow, B., Ramirez, A., Bryda, E. C., Kutsche, K., Nothwang, H. G., Seeliger, M., del, C. S. C. M., Vila, M. C., Molina, O. P., Gal, A., and Kubisch, C. (2001). Mutation of CDH23, encoding a new member of the cadherin gene family, causes Usher syndrome type 1D. *Nat. Genet.* 27, 108–112.
- Brunet, L. J., Gold, G. H., and Ngai, J. (1996). General anosmia caused by a targeted disruption of the mouse olfactory cyclic nucleotide-gated cation channel. *Neuron* 17, 681–693.
- Cao, Y., Zhao, F. L., Kolli, T., Hivley, R., and Herness, S. (2009). GABA expression in the mammalian taste bud functions as a route of inhibitory cell-to-cell communication. *Proc. Natl. Acad. Sci. U.S.A.* 106, 4006–4011.
- Castillon, N., Hinnrasky, J., Zahm, J. M., Kaplan, H., Bonnet, N., Corlieu, P., Klossek, J. M., Taouil, K., Avril-Delplanque, A., Peault, B., and Puchelle, E. (2002). Polarized expression of cystic fibrosis transmembrane conductance regulator and associated epithelial proteins during the regeneration of human airway surface epithelium in three-dimensional culture. *Lab. Invest.* 82, 989–998.
- Cheng, J., Moyer, B. D., Milewski, M., Loffing, J., Ikeda, M., Mickle, J. E., Cutting, G. R., Li, M., Stanton, B. A., and Guggino, W. B. (2002). A Golgi-associated PDZ domain protein modulates cystic fibrosis transmembrane regulator plasma membrane expression. *J. Biol. Chem.* 277, 3520–3529.
- Ciolofan, C., Li, X. B., Olson, C., Kamasawa, N., Gebhardt, B. R., Yasumura, T., Morita, M., Rash, J. E., and Nagy, J. I. (2006). Association of connexin36 and zonula occludens-1 with zonula occludens-2 and the transcription factor zonula occludens-1-associated nucleic acid-binding protein at neuronal gap junctions in rodent retina. *Neuroscience* 140, 433–451.
- Clapp, T. R., Stone, L. M., Margolskee, R. F., and Kinnamon, S. C. (2001). Immunocytochemical evidence for co-expression of Type III IP3 receptor with signaling components of bitter taste transduction. *BMC Neurosci.* 2, 6.
- Clapp, T. R., Trubey, K. R., Vandenbeuch, A., Stone, L. M., Margolskee, R. F., Chaudhari, N., and Kinnamon, S. C. (2008). Tonic activity of Galpha-gustducin regulates taste cell responsiveness. *FEBS Lett.* 582, 3783–3787.
- Dooley, R., Baumgart, S., Rasche, S., Hatt, H., and Neuhaus, E. M. (2009). Olfactory receptor signaling is regulated by the postsynaptic density 95, *Drosophila* discs large, zona-occludens 1 (PDZ) scaffold multi-PDZ domain protein 1. *FEBS J.* 276, 7279–7290.
- Fanning, A. S., Jameson, B. J., Jesaitis, L. A., and Anderson, J. M. (1998). The tight junction protein ZO-1 establishes a link between the transmembrane protein occludin and the actin cytoskeleton. *J. Biol. Chem.* 273, 29745–29753.
- Fanning, A. S., Ma, T. Y., and Anderson, J. M. (2002). Isolation and functional characterization of the actin binding region in the tight junction protein ZO-1. *FASEB J.* 16, 1835–1837.
- Fenech, C., Patrikainen, L., Kerr, D. S., Grall, S., Liu, Z., Laugerette, F., Malnic, B., and Montmayeur, J. P. (2009). Ric-8A, a Galpha protein guanine nucleotide exchange factor potentiates taste receptor signaling. *Front. Cell. Neurosci.* 3:11. doi: 10.3389/neuro.03.011.2009
- Finger, T. E. (2005). Cell types and lineages in taste buds. *Chem. Senses* 30 (Suppl. 1), i54–i55.
- Furuse, M., Fujita, K., Hiiragi, T., Fujimoto, K., and Tsukita, S. (1998). Claudin-1 and -2, novel integral membrane proteins localizing at tight junctions with no sequence similarity to occludin. *J. Cell Biol.* 141, 1539–1550.
- Furuse, M., Itoh, M., Hirase, T., Nagafuchi, A., Yonemura, S., Tsukita, S., and Tsukita, S. (1994).

- Direct association of occludin with ZO-1 and its possible involvement in the localization of occludin at tight junctions. *J. Cell Biol.* 127, 1617–1626.
- Gao, N., Lu, M., Echeverri, F., Laita, B., Kalabat, D., Williams, M. E., Hevezi, P., Zlotnik, A., and Moyer, B. D. (2009). Voltage-gated sodium channels in taste bud cells. *BMC Neurosci.* 10, 20.
- Gentsch, M., Cui, L., Mengos, A., Chang, X. B., Chen, J. H., and Riordan, J. R. (2003). The PDZ-binding chloride channel CIC-3B localizes to the Golgi and associates with cystic fibrosis transmembrane conductance regulator-interacting PDZ proteins. *J. Biol. Chem.* 278, 6440–6449.
- Gilbertson, T. A., Damak, S., and Margolskee, R. F. (2000). The molecular physiology of taste transduction. *Curr. Opin. Neurobiol.* 10, 519–527.
- Gumbiner, B., Lowenkopf, T., and Apatira, D. (1991). Identification of a 160-kDa polypeptide that binds to the tight junction protein ZO-1. *Proc. Natl. Acad. Sci. U.S.A.* 88, 3460–3464.
- Hacker, K., Laskowski, A., Feng, L., Restrepo, D., and Medler, K. (2008). Evidence for two populations of bitter responsive taste cells in mice. *J. Neurophysiol.* 99, 1503–1514.
- Hamazaki, Y., Itoh, M., Sasaki, H., Furuse, M., and Tsukita, S. (2002). Multi-PDZ domain protein 1 (MUPP1) is concentrated at tight junctions through its possible interaction with claudin-1 and junctional adhesion molecule. *J. Biol. Chem.* 277, 455–461.
- Hassel, B., Schreff, M., Stube, E. M., Blaich, U., and Schumacher, S. (2003). CALEB/NGC interacts with the Golgi-associated protein PIST. *J. Biol. Chem.* 278, 40136–40143.
- He, W., Yasumatsu, K., Varadarajan, V., Yamada, A., Lem, J., Ninomiya, Y., Margolskee, R. F., and Damak, S. (2004). Umami taste responses are mediated by alpha-transducin and alpha-gustducin. *J. Neurosci.* 24, 7674–7680.
- Hofer, D., and Drenkhahn, D. (1999). Localisation of actin, villin, fimbrin, ezrin and ankyrin in rat taste receptor cells. *Histochem. Cell Biol.* 112, 79–86.
- Huang, L., Max, M., Margolskee, R. F., Su, H., Masland, R. H., and Euler, T. (2003). G protein subunit G gamma 13 is coexpressed with G alpha o, G beta 3, and G beta 4 in retinal ON bipolar cells. *J. Comp. Neurol.* 455, 1–10.
- Huang, L., Shanker, Y. G., Dubauskaite, J., Zheng, J. Z., Yan, W., Rosenzweig, S., Spielman, A. I., Max, M., and Margolskee, R. F. (1999). Ggamma13 colocalizes with gustducin in taste receptor cells and mediates IP3 responses to bitter denatonium. *Nat. Neurosci.* 2, 1055–1062.
- Huang, Y. A., and Roper, S. D. (2010). Intracellular Ca(2+) and TRPM5-mediated membrane depolarization produce ATP secretion from taste receptor cells. *J. Physiol.* 588, 2343–2350.
- Ito, H., Iwamoto, I., Morishita, R., Nozawa, Y., Asano, T., and Nagata, K. (2006). Identification of a PDZ protein, PIST, as a binding partner for Rho effector Rhotekin: biochemical and cell-biological characterization of Rhotekin-PIST interaction. *Biochem. J.* 397, 389–398.
- Itoh, M., Furuse, M., Morita, K., Kubota, K., Saitou, M., and Tsukita, S. (1999). Direct binding of three tight junction-associated MAGUKs, ZO-1, ZO-2, and ZO-3, with the COOH termini of claudins. *J. Cell Biol.* 147, 1351–1363.
- Kalyoncu, S., Keskin, O., and Gursoy, A. (2010). Interaction prediction and classification of PDZ domains. *BMC Bioinformatics* 11, 357.
- Kerr, D. S., von Dannecker, L. E., Davalos, M., Michaloski, J. S., and Malnic, B. (2008). Ric-8B interacts with G alpha olf and G gamma 13 and co-localizes with G alpha olf, G beta 1 and G gamma 13 in the cilia of olfactory sensory neurons. *Mol. Cell. Neurosci.* 38, 341–348.
- Kim, J. H., Kim, J. H., Yu, Y. S., Kim, D. H., and Kim, K. W. (2009). Recruitment of pericytes and astrocytes is closely related to the formation of tight junction in developing retinal vessels. *J. Neurosci. Res.* 87, 653–659.
- Kulaga, H. M., Leitch, C. C., Eichers, E. R., Badano, J. L., Lesemann, A., Hoskins, B. E., Lupski, J. R., Beales, P. L., Reed, R. R., and Katsanis, N. (2004). Loss of BBS proteins causes anosmia in humans and defects in olfactory cilia structure and function in the mouse. *Nat. Genet.* 36, 994–998.
- Kusakabe, Y., Yasuoka, A., Asano-Miyoshi, M., Iwabuchi, K., Matsumoto, I., Arai, S., Emori, Y., and Abe, K. (2000). Comprehensive study on G protein alpha-subunits in taste bud cells, with special reference to the occurrence of Galpha2 as a major Galpha species. *Chem. Senses* 25, 525–531.
- Lee, A. C., He, J., and Ma, M. (2011). Olfactory marker protein is critical for functional maturation of olfactory sensory neurons and development of mother preference. *J. Neurosci.* 31, 2974–2982.
- Li, Z., Benard, O., and Margolskee, R. F. (2006). Ggamma13 interacts with PDZ domain-containing proteins. *J. Biol. Chem.* 281, 11066–11073.
- Liew, C. W., Vockel, M., Glassmeier, G., Brandner, J. M., Fernandez-Ballester, G. J., Schwarz, J. R., Schulz, S., Buck, F., Serrano, L., Richter, D., and Kreienkamp, H. J. (2009). Interaction of the human somatostatin receptor 3 with the multiple PDZ domain protein MUPP1 enables somatostatin to control permeability of epithelial tight junctions. *FEBS Lett.* 583, 49–54.
- Matsunami, H., Montmayeur, J. P., and Buck, L. B. (2000). A family of candidate taste receptors in human and mouse. *Nature* 404, 601–604.
- McEwen, D. P., Koenekoop, R. K., Khanna, H., Jenkins, P. M., Lopez, L., Swaroop, A., and Martens, J. R. (2007). Hypomorphic CEP290/NPHP6 mutations result in anosmia caused by the selective loss of G proteins in cilia of olfactory sensory neurons. *Proc. Natl. Acad. Sci. U.S.A.* 104, 15917–15922.
- McLaughlin, S. K., McKinnon, P. J., and Margolskee, R. F. (1992). Gustducin is a taste-cell-specific G protein closely related to the transducins. *Nature* 357, 563–569.
- Meyer, T. N., Schwesinger, C., and Denker, B. M. (2002). Zonula occludens-1 is a scaffolding protein for signaling molecules. Galpha(12) directly binds to the Src homology 3 domain and regulates paracellular permeability in epithelial cells. *J. Biol. Chem.* 277, 24855–24858.
- Michlig, S., Damak, S., and Le Coutre, J. (2007). Claudin-based permeability barriers in taste buds. *J. Comp. Neurol.* 502, 1003–1011.
- Miragall, F., Krause, D., de Vries, U., and Dermietzel, R. (1994). Expression of the tight junction protein ZO-1 in the olfactory system: presence of ZO-1 on olfactory sensory neurons and glial cells. *J. Comp. Neurol.* 341, 433–448.
- Mitic, L. L., and Anderson, J. M. (1998). Molecular architecture of tight junctions. *Annu. Rev. Physiol.* 60, 121–142.
- Ohtubo, Y., and Yoshii, K. (2011). Quantitative analysis of taste bud cell numbers in fungiform and soft palate taste buds of mice. *Brain Res.* 1367, 13–21.
- Ozeck, M., Brust, P., Xu, H., and Servant, G. (2004). Receptors for bitter, sweet and umami taste couple to inhibitory G protein signaling pathways. *Eur. J. Pharmacol.* 489, 139–149.
- Poon, L. S., Chan, A. S., and Wong, Y. H. (2009). Gbeta3 forms distinct dimers with specific Ggamma subunits and preferentially activates the beta3 isoform of phospholipase C. *Cell. Signal.* 21, 737–744.
- Ren, X., Zhou, L., Terwilliger, R., Newton, S. S., and de Araujo, I. E. (2009). Sweet taste signaling functions as a hypothalamic glucose sensor. *Front. Integr. Neurosci.* 3:12. doi: 10.3389/fneuro.07.012.2009
- Rossler, P., Boekhoff, I., Tareilus, E., Beck, S., Breer, H., and Freitag, J. (2000). G protein betagamma complexes in circumvallate taste cells involved in bitter transduction. *Chem. Senses* 25, 413–421.
- Sabath, E., Negoro, H., Beaudry, S., Paniagua, M., Angelow, S., Shah, J., Grammatikakis, N., Yu, A. S., and Denker, B. M. (2008). Galpha12 regulates protein interactions within the MDCK cell tight junction and inhibits tight-junction assembly. *J. Cell Sci.* 121, 814–824.
- Saha, C., Nigam, S. K., and Denker, B. M. (2001). Expanding role of G proteins in tight junction regulation: Galpha(s) stimulates TJ assembly. *Biochem. Biophys. Res. Commun.* 285, 250–256.
- Sainz, E., Cavenagh, M. M., Gutierrez, J., Battey, J. F., Northup, J. K., and Sullivan, S. L. (2007). Functional characterization of human bitter taste receptors. *Biochem. J.* 403, 537–543.
- Schwarzenbacher, K., Fleischer, J., and Breer, H. (2005). Formation and maturation of olfactory cilia monitored by odorant receptor-specific antibodies. *Histochem. Cell Biol.* 123, 419–428.
- Sheng, M. (1996). PDZs and receptor/channel clustering: rounding up the latest suspects. *Neuron* 17, 575–578.
- Steinke, A., Meier-Stiegen, S., Drenkhahn, D., and Asan, E. (2008). Molecular composition of tight and adherens junctions in the rat olfactory epithelium and fila. *Histochem. Cell Biol.* 130, 339–361.
- Stevenson, B. R., and Keon, B. H. (1998). The tight junction: morphology to molecules. *Annu. Rev. Cell Dev. Biol.* 14, 89–109.

- Takeda, M., Obara, N., and Suzuki, Y. (1989). Cytoskeleton in the apical region of mouse taste bud cells. *Shika Kiso Igakkai Zasshi* 31, 317–323.
- Tsukita, S., and Furuse, M. (1998). Overcoming barriers in the study of tight junction functions: from occludin to claudin. *Genes Cells* 3, 569–573.
- Tsukita, S., Yamazaki, Y., Katsuno, T., Tamura, A., and Tsukita, S. (2008). Tight junction-based epithelial microenvironment and cell proliferation. *Oncogene* 27, 6930–6938.
- Utepergenov, D. I., Fanning, A. S., and Anderson, J. M. (2006). Dimerization of the scaffolding protein ZO-1 through the second PDZ domain. *J. Biol. Chem.* 281, 24671–24677.
- Vandenbeuch, A., and Kinnamon, S. C. (2009). Why do taste cells generate action potentials? *J. Biol.* 8, 42.
- Wente, W., Stroh, T., Beaudet, A., Richter, D., and Kreienkamp, H. J. (2005). Interactions with PDZ domain proteins PIST/GOPC and PDZK1 regulate intracellular sorting of the somatostatin receptor subtype 5. *J. Biol. Chem.* 280, 32419–32425.
- Wong, G. T., Gannon, K. S., and Margolskee, R. F. (1996). Transduction of bitter and sweet taste by gustducin. *Nature* 381, 796–800.
- Wong, S. T., Trinh, K., Hacker, B., Chan, G. C., Lowe, G., Gaggar, A., Xia, Z., Gold, G. H., and Storm, D. R. (2000). Disruption of the type III adenylyl cyclase gene leads to peripheral and behavioral anosmia in transgenic mice. *Neuron* 27, 487–497.
- Xu, Z., Oshima, K., and Heller, S. (2010). PIST regulates the intracellular trafficking and plasma membrane expression of Cadherin 23. *BMC Cell Biol.* 11, 80.
- Yao, R., Maeda, T., Takada, S., and Noda, T. (2001). Identification of a PDZ domain containing Golgi protein, GOPC, as an interaction partner of frizzled. *Biochem. Biophys. Res. Commun.* 286, 771–778.
- Zhang, Y., Hoon, M. A., Chandrashekar, J., Mueller, K. L., Cook, B., Wu, D., Zuker, C. S., and Ryba, N. J. (2003). Coding of sweet, bitter, and umami tastes: different receptor cells sharing similar signaling pathways. *Cell* 112, 293–301.
- Zitanski, N., Borth, H., Ackermann, F., Meyer, D., Viewig, L., Breit, A., Gudermann, T., and Boekhoff, I. (2010). The “acrosomal synapse”: subcellular organization by lipid rafts and scaffolding proteins exhibits high similarities in neurons and mammalian spermatozoa. *Commun. Integr. Biol.* 3, 513–521.
- that could be construed as a potential conflict of interest.

Received: 03 April 2012; paper pending published: 13 April 2012; accepted: 31 May 2012; published online: 21 June 2012.

Citation: Liu Z, Fenech C, Cadiou H, Grall S, Tili E, Laugerette F, Wiencis A, Grosmaître X and Montmayeur J-P (2012) Identification of new binding partners of the chemosensory signaling protein G $\gamma$ 13 expressed in taste and olfactory sensory cells. *Front. Cell. Neurosci.* 6:26. doi: 10.3389/fncel.2012.00026

Copyright © 2012 Liu, Fenech, Cadiou, Grall, Tili, Laugerette, Wiencis, Grosmaître and Montmayeur. This is an open-access article distributed under the terms of the Creative Commons Attribution Non Commercial License, which permits non-commercial use, distribution, and reproduction in other forums, provided the original authors and source are credited.

**Conflict of Interest Statement:** The authors declare that the research was conducted in the absence of any commercial or financial relationships

## APPENDIX

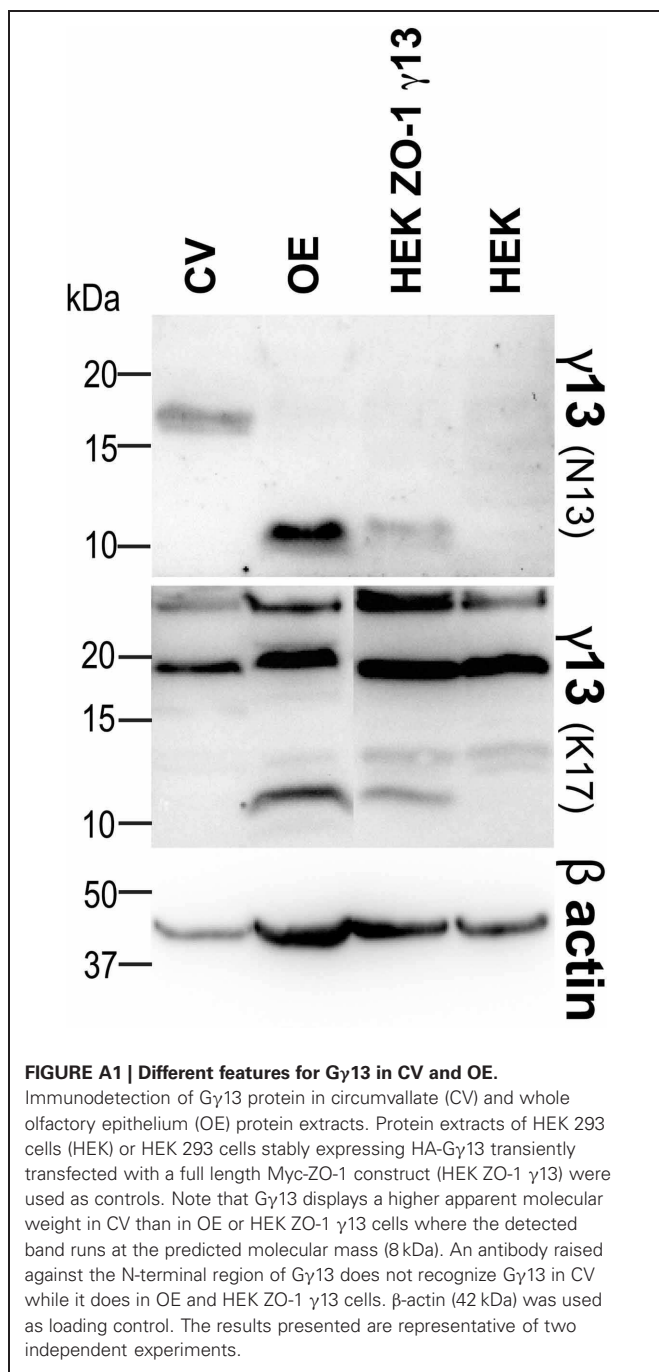


**FIGURE A1 | Different features for Gy13 in CV and OE.**

Immunodetection of Gy13 protein in circumvallate (CV) and whole olfactory epithelium (OE) protein extracts. Protein extracts of HEK 293 cells (HEK) or HEK 293 cells stably expressing HA-Gy13 transiently transfected with a full length Myc-ZO-1 construct (HEK ZO-1  $\gamma$ 13) were used as controls. Note that Gy13 displays a higher apparent molecular weight in CV than in OE or HEK ZO-1  $\gamma$ 13 cells where the detected band runs at the predicted molecular mass (8 kDa). An antibody raised against the N-terminal region of Gy13 does not recognize Gy13 in CV while it does in OE and HEK ZO-1  $\gamma$ 13 cells.  $\beta$ -actin (42 kDa) was used as loading control. The results presented are representative of two independent experiments.

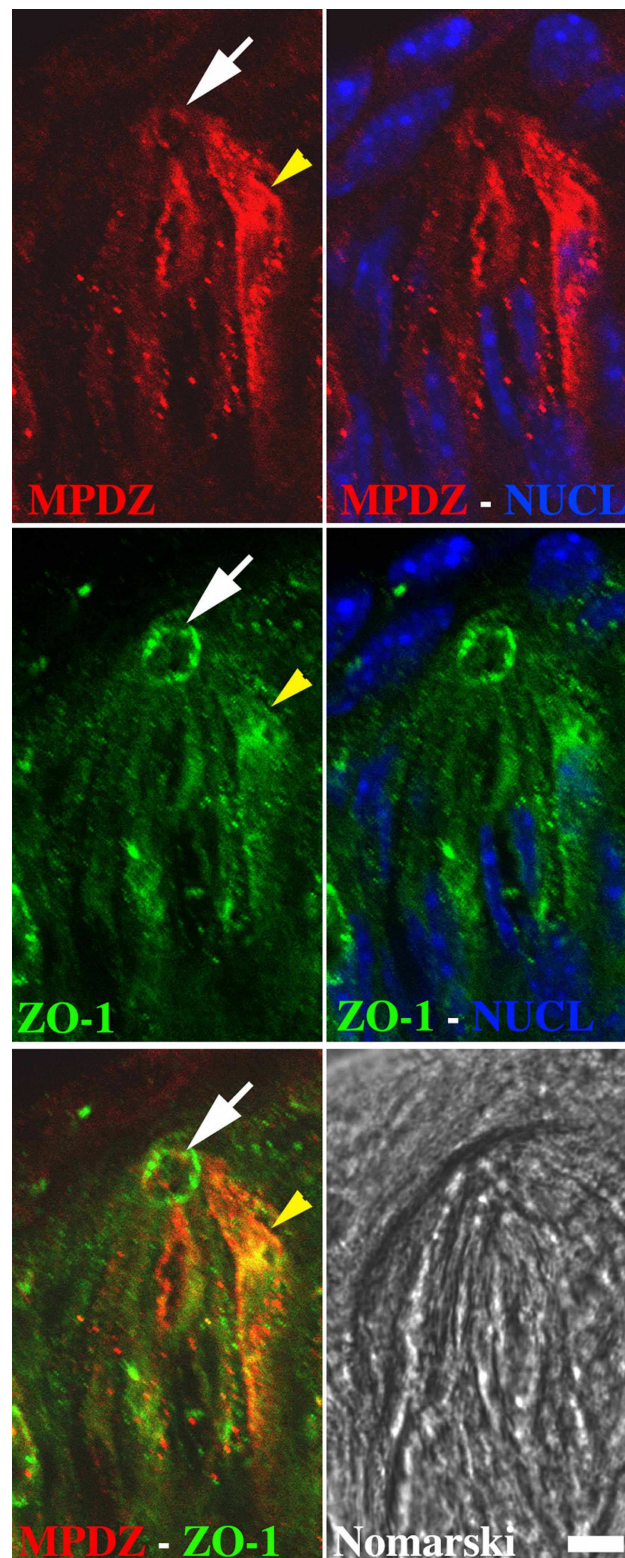


**FIGURE A2 | Partial co-localization between ZO-1 and MPDZ in CV taste bud cells.** Immunolocalization of MPDZ (red) and ZO-1 (green) in circumvallate taste buds. Indirect immunofluorescence on saggital cryosections of circumvallate papillae was performed as described under Section "Immunohistochemistry." Each image shows one entire taste

bud (apical: up, basal: down). Nuclei (blue) were visualized using nuclear stain. MPDZ and ZO-1 staining overlaps partly in the cytoplasm (yellow arrowhead) and at the taste pore (white arrow). The Nomarski image shows the location of the taste bud. Scale bar = 15  $\mu$ m. Images are representative of staining patterns from at least 5 taste buds.

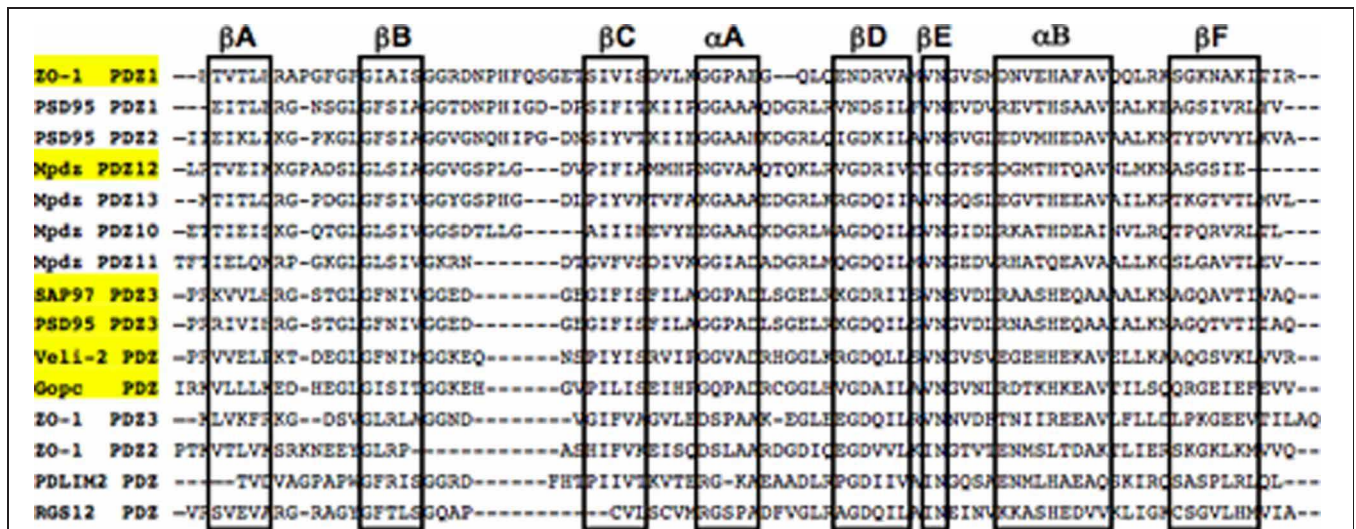


**FIGURE A3 | PDZ domains sequence alignment.** The amino acid sequence of select PDZ domains from GOPC, MPDZ, PDLIM2, PSD95, RGS12, SAP97, and Veli-2 used in our initial yeast-two hybrid screening were aligned using clustalW 2.1. Residues involved in  $\alpha$ -helices and  $\beta$ -sheet structures are boxed.

PDZ domains interacting with Gy13 are highlighted in yellow. Note that the stretch of amino acids present between the  $\beta$ B and  $\beta$ C sheet is of variable length between the various binding partners of Gy13 thus making it unlikely that this region plays a critical role in the interaction as suggested by Li et al.

**Table A1 | List of primer sequences and corresponding annealing temperatures used for PCR experiments.**

Gene	Forward primer sequence	Reverse primer sequence	Template Acc#	Ampl. size (bp)	T <sub>m</sub> (°C)
Gng13	CGAGGTCGACTGAGGAGTGGGATGTGCC	CTTAGCGGCCGCTCATAGGATGGTGCACTT	AY029485	200	56
Gng13TA	CGAGGTCGACTGAGGAGTGGGATGTGCC	CTTAGCGGCCGCTCATAGGATGGCGCACTT	AY029485	200	54
Tjp1 (PDZ1)	CGAGGTCGACTGCAATGGAGGAAACAGCTA	CTTAGCGGCCGCTTAACCTACAGGGATCTGAACTTTC	BC138028	317	58
Tjp1 (PDZ2)	CGAGGTCGACTTCCGTGGCCTCCAGTCAG	CTTAGCGGCCGCTTAAATTTCTGAAATGTCATCTCTTTCC	BC138028	353	58
Tjp1 (PDZ3)	CGAGGTCGACTCCGAAACCTGTGTATGCT	CTTAGCGGCCGCTTAAACGTCTTCTTTCTG	BC138028	365	55
#Tjp1 (PDZ1-2)	CGAGGTCGACTGCAATGGAGGAAACAGCTA	CTTAGCGGCCGCTTAAATTTCTGAAATGTCATCTCTTTCC	BC138028	842	58
Tjp1 (PDZ2-3)	CGAGGTCGACTTCCGTGGCCTCCAGTCAG	CTTAGCGGCCGCTTAAACGTCTTCTTTCTG	BC138028	995	55
Tjp1 (PDZ3-SH3)	CGAGGTCGACTCCGAAACCTGTGTATGCT	CTTAGCGGCCGCTTAAGCTGGGAACTAGTTTGAA	BC138028	743	56
Tjp1 (SH3)	CGAGGTCGACTGTGACCATACTGGCTCAG	CTTAGCGGCCGCTTAAGCTGGGAACTAGTTTGAA	BC138028	410	56
Tjp1 (PDZ1-SH3)	CGAGGTCGACTGCAATGGAGGAAACAGCTA	CTTAGCGGCCGCTTAAGCTGGGAACTAGTTTGAA	BC138028	1862	56
Tjp1 (PDZ1-PDZ3)	CGAGGTCGACTGCAATGGAGGAAACAGCTA	CTTAGCGGCCGCTTAAACGTCTTCTTTCTG	BC138028	1484	55
Cldn1	CGAGGTCGACTCGAAAACACCTCTTAC	CTTAGCGGCCGCTCACACATAGTCTTTCCC	EU076705	74	55
Cldn4	CGAGGTCGACTCCTCGTAGCAACGACAAG	CTTAGCGGCCGCTTACACATAGTTGCTGGCGG	AF087822	74	60
Cldn8	CGAGGTCGACTACTGAAAGGAGCAACAGTTA	CTTAGCGGCCGCTTACACATACTGACTTTTGG	AF087826	113	56
F11r	CGAGGTCGACCAGCCGTGGATACTTTGAAAGAAC	CTTAGCGGCCGCTCACACCAGGAACGACGA	BC021876	119	60
Lin7b	CGAGGTCGACTCCCAGGGTCGTGGAACCTA	CTTAGCGGCCGCTCAAGTGTAGCGCACCACCAG	AF087694	251	62
Dlg1 (PDZ3)	CGAGGTCGACTATCACTAGGGAACCTAGA	CTTAGCGGCCGCTTAACTGACTGTACTTTCGGG	AY159380	279	55
Dlg4 (PDZ3)	CGAGGTCGACTAGGCGGATCGTGATCCAT	CTTAGCGGCCGCTTACTTCTGTTTATACTGAGC	BC014807	256	58
Mpdz (PDZ10-11)	CGAGGTCGACTTCTCCACACCAGCAGTC	CTTAGCGGCCGCTTAGGGGGAGTGAAAGATGACAG	BC145117	682	62
#Mpdz (PDZ12-13)	CGAGGTCGACTGGAATAAATACATCAGAGTCA	CTTAGCGGCCGCTCAAGAGAGAACCATGAG	BC145117	704	55
Pdlim2	CGAGGTCGACTATGGCGTTGACTGTGGATG	CTTAGCGGCCGCTTATGTTTGGGACCGTCCAG	BC024556	254	60
#Gopc	CGAGGTCGACTATTAGAAAAGTTCTCCTCCTT	CTTAGCGGCCGCTTAGACTACTTCAAACCTCAATC	AF287894	250	54
Rgs12	CGAGGTCGACTGTGCGGAGCGTCGAAGTG	CTTAGCGGCCGCTCACTCAGCAATCACCATGTGCAG	BC40396	233	62
*Gng13	ATGGAGGAGTGGGATGT	TCATAGGATGGTGCACTTG	AY029485	203	54
*Gnat3	TCAGGAGGATGCTGAGCG	ATGCCCTTCAAAGCAGGC	BC147841	361	56
*Gapdh	TGTCACCCAGGGCTGC	GTGGCAGTGATGGCATG	GU214026	501	59

(\* ) Primers and annealing temperatures used for RT-PCR only.

(#) Primers and annealing temperatures used for both cloning and RT-PCR experiments.

(Acc#) GenBank accession number.

**Table A2 | Table summarizing the results (from at least three independent experiments) of the yeast two-hybrid interaction assays performed with different combinations of baits and preys.**

Bait	Prey	3-AT (12.5 mM)	3-AT (25 mM)	3-AT (50 mM)
Gy13	ZO-1 PDZ1	+	+	–
Gy13	ZO-1 PDZ2	+	–	
Gy13	ZO-1 PDZ3	–		
Gy13	ZO-1 SH3	+	–	
Gy13	ZO-1 PDZ1-2	+	+	+
Gy13	ZO-1 PDZ2-3	+	–	
Gy13	ZO-1 PDZ3-SH3	+	–	
Gy13	ZO-1 PDZ1-2-3-SH3	+	+	
Gy13	Veli-2	+	–	
Gy13	PSD95 PDZ3	+	–	
Gy13	SAP97 PDZ3	+	–	
Gy13	PDLIM2	–		
Gy13	GOPC	+	+	
Gy13	RGS12	+	–	
Gy13	MPDZ PDZ10-11	+	–	
Gy13	MPDZ PDZ12-13	+	+	
Gy13*	ZO-1 PDZ1	–		
Gy13*	ZO-1 PDZ1-2	–		
Gy13*	GOPC	–		
Gy13*	MPDZ PDZ12-13	–		
Claudin 1	ZO-1 PDZ1	–		
Claudin 1	ZO-1 PDZ2	–		
Claudin 1	ZO-1 PDZ3	–		
Claudin 1	ZO-1 PDZ1-2	+	–	
Claudin 1	ZO-1 PDZ3-SH3	–		
Claudin 1	MPDZ PDZ8-9	+	–	
Claudin 1	MPDZ PDZ10-11	+	–	
Claudin 1	MPDZ PDZ12-13	–		
Claudin 4	ZO-1 PDZ1	–		
Claudin 4	ZO-1 PDZ2	–		
Claudin 4	ZO-1 PDZ3	–		
Claudin 4	ZO-1 PDZ1-2	+	+	–
Claudin 4	ZO-1 PDZ3-SH3	–		
Claudin 4	MPDZ PDZ8-9	+	–	
Claudin 4	MPDZ PDZ10-11	+	–	
Claudin 4	MPDZ PDZ12-13	–		
Claudin 8	ZO-1 PDZ1	+	+	+
Claudin 8	ZO-1 PDZ2	–		
Claudin 8	ZO-1 PDZ3	–		
Claudin 8	ZO-1 PDZ1-2	+	+	+
Claudin 8	ZO-1 PDZ3-SH3	–		
Claudin 8	MPDZ PDZ8-9	+	–	
Claudin 8	MPDZ PDZ10-11	+	–	
Claudin 8	MPDZ PDZ12-13	–		
JAM	ZO-1 PDZ3	–		
JAM	ZO-1 PDZ1-2	–		
JAM	ZO-1 PDZ2-3	–		
JAM	ZO-1 PDZ3-SH3	–		

The strength of the interaction was assessed by analyzing growth at 30°C in the presence of increasing concentrations of 3-AT. (+) indicates growth (–) indicates absence of growth. Cells were left empty when the experiment was not performed. Gy13\* is for the T65A mutant. JAM: Junctional adhesion molecule 1.